

METHODS FOR TARGET DETECTION IN SAR IMAGES

A THESIS

SUBMITTED TO THE DEPARTMENT OF ELECTRICAL AND
ELECTRONICS ENGINEERING

AND THE INSTITUTE OF ENGINEERING AND SCIENCE
OF BILKENT UNIVERSITY

IN PARTIAL FULFILLMENT OF THE REQUIREMENTS

FOR THE DEGREE OF

MASTER OF SCIENCE

By

Kaan Duman

December 2009

I certify that I have read this thesis and that in my opinion it is fully adequate, in scope and in quality, as a thesis for the degree of Master of Science.

Prof. Dr. A. Enis Çetin(Supervisor)

I certify that I have read this thesis and that in my opinion it is fully adequate, in scope and in quality, as a thesis for the degree of Master of Science.

Prof. Dr. Ömer Morgül

I certify that I have read this thesis and that in my opinion it is fully adequate, in scope and in quality, as a thesis for the degree of Master of Science.

Assoc. Prof. Dr. Uğur Güdükbay

Approved for the Institute of Engineering and Science:

Prof. Dr. Mehmet Baray
Director of the Institute

ABSTRACT

METHODS FOR TARGET DETECTION IN SAR IMAGES

Kaan Duman

M.S. in Electrical and Electronics Engineering

Supervisor: Prof. Dr. A. Enis Çetin

December 2009

Automatic recognition and classification of man-made objects in SAR (Synthetic Aperture Radar) images have been an active research area because SAR sensors can produce images of scenes in all weather conditions at any time of the day which is not possible with infrared and optical sensors [1, 2]. In this thesis, different feature parameter extraction methods from SAR images are proposed. The new approach is based on region covariance (RC) method which involves the computation of a covariance matrix of a ROI (region of interest). Entries of the covariance matrix are used in target detection. In addition, the use of computationally more efficient region codifference matrix for target detection in SAR images is also introduced. Simulation results of target detection in MSTAR (Moving and Stationary Target Recognition) database are presented. The RC and region codifference methods deliver high detection accuracies and low false alarm rates. The performance of these methods is investigated with various distance metrics and Support Vector Machine (SVM) classifiers. It is also observed that the region codifference method produces better results than the commonly used Principle Component Analysis (PCA) method which is used together with SVM.

The second part of the thesis offers some techniques to decrease the computational cost of the proposed methods. In this approach, ROIs are filtered by directional filters (DFs) at first as a pre-processing stage. Images are categorized according to the filter outputs. The proposed RC and codifference methods are applied within the categories determined by these filters. Simulation results of target detection in MSTAR database are presented through decisions made with l_1 norm distance metric and SVM. The number of comparisons made with the training images using l_1 norm distance measure decreases as these images are distributed into categories. Therefore, the computational cost of the previous algorithm is significantly reduced. SAR image classification results based on l_1 norm distance metric are better than the results obtained using SVM and they show that the two-stage approach does not reduce the performance rate of the previously proposed method much, especially when codifference features are used.

Keywords: Synthetic Aperture Radar (SAR) images, Automatic Target Recognition (ATR) and Classification, region covariance (RC), region codifference matrix, directional filters (DFs), Support Vector Machines (SVM), Principal Component Analysis (PCA)

ÖZET

SAR İMGELERİNDE HEDEF TESPİT YÖNTEMLERİ

Kaan Duman

Elektrik ve Elektronik Mühendisliği Bölümü Yüksek Lisans

Tez Yöneticisi: Prof. Dr. A. Enis Çetin

Aralık 2009

SAR (Sentetik Açıklık Radarı) imgelerinde insan yapımı nesnelerin otomatik tanıma ve sınıflandırması aktif bir araştırma alanı oluşturmuştur, çünkü kızılötesi ve optik algılayıcıların aksine SAR algılayıcıları günün her saatinde ve her türlü hava şartlarında imge üretebilmektedir [1, 2]. Bu tezde, SAR imgelerinden çeşitli öznitelik parametre çıkarma yöntemleri sunulmaktadır. Bu yeni yaklaşım bir ilgi bölgesinin (ROI) ortak değişinti matrisinin hesaplanmasını içeren bölge ortak değişinti (RC) yöntemine dayanmaktadır. Ortak değişinti matrisinin elemanları hedef tespitte kullanılmıştır. Ayrıca, SAR imgelerinde hedef tespiti için hesaplama yükü açısından daha verimli olan bölge ortak fark matrisi de tanıtılmıştır. MSTAR (Hareketli ve Durağan Hedef Tanıma) veritabanı üzerinde hedef tespit benzetim sonuçları verilmiştir. Bölge ortak değişinti ve fark yöntemleri yüksek tespit doğrulukları ve düşük yanlış kabul yüzdeleri ortaya koymaktadır. Bu yöntemlerin performansları çeşitli uzaklık metrikleri ve Destekçi Vektör Makine (SVM) sınıflandırıcıları kullanılarak incelenmiştir. Aynı zamanda, benzetim sonuçlarına bakıldığında, bölge ortak fark yönteminin yaygın olarak uygulanan ve burada SVM ile birlikte kullanılan Temel Bileşenler Analizi (PCA) yöntemine göre daha iyi sonuçlar verdiği gözlemlenmiştir.

Tezin ikinci bölümünde, önerilen yöntemlerin hesaplama yükünü azaltmak için yeni teknikler öne sürülmektedir. Bu yaklaşımda, bir önışleme kademesi olarak imge bölgeleri yön süzgeçlerinden (DFs) geçirilmiştir. Önerilen ortak deęişinti ve fark yöntemleri, bu süzgeçler aracılığıyla belirlenen kategoriler içerisinde uygulanmıştır. MSTAR veritabanında l_1 düzge uzaklık metrięi ve SVM kullanılarak alınan kararlar doęrultusunda hedef tespit benzetim sonuçları ortaya konulmuştur. Eğitim imgelerinin kategorilere ayrılmasından dolayı, l_1 düzge uzaklık ölçütü kullanıldığında bu imgelerle yapılan karşılaştırma sayısı azalmaktadır. Bu sayede, önceki algoritmanın hesaplama yükü büyük ölçüde düşer. Uzaklık ölçütü olarak l_1 düzgeye dayalı SAR imge sınıflandırması sonuçları SVM kullanılarak elde edilen sonuçlara göre daha iyidir. Ayrıca bu sonuçlar, özellikle ortak fark öznelikleri kullanıldığında, iki-kademeli sistemin hedef tespit performansının önerilen önceki yöntemle göre fazla düşmediğini göstermiştir.

Anahtar Kelimeler: Sentetik Açıklık Radarı (SAR) imgeleri, Otomatik Hedef Tanıma (ATR) ve Sınıflandırması, bölge ortak deęişinti (RC), bölge ortak fark matrisi, yön süzgeçleri (DFs), Destekçi Vektör Makineleri (SVM), Temel Bileşenler Analizi (PCA)

ACKNOWLEDGMENTS

I would like to express my gratitude to Prof. Dr. A. Enis etin for his supervision, suggestions and encouragement throughout the development of this thesis.

I am also indebted to Prof. Dr. mer Morgl and Assoc. Prof. Dr. Uğur Gdkbay for accepting to read and review this thesis.

I wish to thank my family, my friends and my colleagues at our department for their support and collaboration.

I would also like to thank TBİTAK for funding the work presented in this thesis with MİLDAR Project (No. 107A011).

Contents

1	Introduction	1
1.2	Feature extraction from SAR images	3
1.3	Thesis Outline	4
2	Target Detection in SAR Images Using Region Covariance (RC) and Codifference	6
2.1	Related Work on Region Covariance (RC) Method	8
2.2	Region Covariance (RC) Matrix	9
2.3	Region Codifference Matrix	11
2.4	The Moving and Stationary Target Recognition SAR Database . .	12
2.5	Stages of the Target Detection Algorithm	15
2.6	Simulation Results	18
2.6.1	Using Various Distance Metrics and Support Vector Machine (SVM) Classifiers	19
2.6.2	Using Principal Component Analysis (PCA) Method	28

2.7	Summary	31
3	Use of Directional Filters (DFs) on Target Detection Methods	32
3.1	Introduction	32
3.2	Pre-processing Stage and Directional Filter (DF) Design	34
3.3	Target Detection Strategy	37
3.4	Simulation Results	38
3.4.1	Using k-Nearest Neighbor (k-NN) Algorithm	51
3.5	Summary	54
4	Conclusions	55

List of Figures

1.1	Synthetic aperture radar (SAR) working principle (adopted from [3]).	2
1.2	Block diagram of a typical SAR ATR (Automatic Target Recognition) system.	3
2.1	Block diagram of three-stage baseline SAR ATR system proposed by Novak et al. [4].	8
2.2	DHC-6 Twin Otter Aircraft which carries Sandia National Laboratories Twin Otter SAR sensor (adopted from [3]).	13
2.3	A sample for X band SAR image collected in DARPA Moving and Stationary Target Recognition (MSTAR) program.	13
2.4	Targets in the MSTAR: (a) BMP-2 Armored Personal Carrier, (b) BTR-70 Armored Personal Carrier, (c) T-72 Main Battle Tank [5].	14
2.5	Several target and clutter images: (a) Target images of size 128-by-128, (b) Clutter images of size 128-by-128.	15
2.6	Block diagram showing stages of the target detection algorithm. .	16
2.7	A sample covariance or codifference matrix where the bounded region shows the necessary features for the decision algorithm. . .	17

2.8	Examples of 128-by-128 and 64-by-64 target and clutter images (ROIs). 64-by-64 images are cropped from the 128-by-128 images.	18
2.9	The target detection accuracies (%) obtained with various decision techniques using (a) RC and (b) codifference methods proposed.	24
2.10	The false alarm rates (%) obtained with various decision techniques using (a) RC and (b) codifference methods proposed.	25
2.11	The target detection accuracies (%) obtained for increasing k values using l_1 norm distance metric.	27
2.12	The false alarm rates (%) obtained for increasing k values using l_1 norm distance metric.	27
3.1	Block diagram of the two-stage target detection process investigated in this chapter	33
3.2	Design of the directional filters (DFs)	35
3.3	Block diagram of the pre-processing stage	36
3.4	Block diagram of the target detection stage applied in each category using (a) l_1 norm distance metric in Eq. 3.1 (b) SVM classifiers.	38
3.5	Example 64-by-64 target images selected by DFs 1 - 10	39
3.6	(a) Target detection accuracies (%) and (b) false alarm rates (%) obtained with the two-stage methods working on 10 categories	41
3.7	(a) Target detection accuracies (%) and (b) false alarm rates (%) obtained with the two-stage methods working on 8 categories	42
3.8	(a) Target detection accuracies (%) and (b) false alarm rates (%) obtained with the two-stage methods working on 7 categories	43

3.9	(a) Target detection accuracies (%) and (b) false alarm rates (%) obtained with the two-stage methods working on 6 categories . . .	44
3.10	(a) Target detection accuracies (%) and (b) false alarm rates (%) obtained with the two-stage methods working on 5 categories . . .	45
3.11	(a) Target detection accuracies (%) and (b) false alarm rates (%) obtained with the two-stage methods working on 4 categories . . .	47
3.12	(a) Target detection accuracies (%) and (b) false alarm rates (%) obtained with the two-stage methods working on 3 categories . . .	48
3.13	(a) Target detection accuracies (%) and (b) false alarm rates (%) obtained with the two-stage methods working on 2 categories . . .	49
3.14	The total target detection accuracies (%) obtained with the two- stage RC and codifference methods using various decision tech- niques on different numbers of categories	50
3.15	The total false alarm rates (%) obtained with the two-stage RC and codifference methods using various decision techniques on dif- ferent numbers of categories	50
3.16	(a) Target detection accuracies (%) and (b) false alarm rates (%) obtained with the two-stage methods working on 10 categories of the new database	52
3.17	The total target detection accuracies (%) obtained for increasing k values on 10 categories for the two-stage system using l_1 norm distance metric.	53
3.18	The total false alarm rates (%) obtained for increasing k values on 10 categories for the two-stage system using l_1 norm distance metric.	53

List of Tables

2.1	Number of images used in training and testing studies	19
2.2	Target detection accuracies and false alarm rates achieved using RC and region codifference methods with the distance metric defined in Eq. 2.7	20
2.3	Target detection accuracies and false alarm rates achieved using RC and region codifference methods with the distance metric defined in Eq. 2.8	20
2.4	Target detection accuracies and false alarm rates achieved using RC and region codifference methods with the distance metric defined in Eq. 2.9	21
2.5	Target detection accuracies and false alarm rates achieved using RC and region codifference methods with the distance metric defined in Eq. 2.10	22
2.6	Target detection accuracies and false alarm rates achieved using RC and region codifference methods with the distance metric defined in Eq. 2.11	22
2.7	Target detection accuracies and false alarm rates achieved using SVM as a classifier	23

2.8	The target detection accuracies and false alarm rates obtained with various numbers of training images	26
2.9	Number of images used in training and testing studies for the PCA method	29
2.10	Target detection accuracies and false alarm rates achieved using PCA method	29
2.11	Target detection accuracies and false alarm rates achieved using the distance metric defined in Eq. 2.9	30
2.12	Target detection accuracies and false alarm rates achieved using SVM as a classifier	30
3.1	Number of training and test images used for the two-stage methods working on 10 categories	40
3.2	Number of training and test images used for the two-stage methods working on 8 categories	42
3.3	Number of training and test images used for the two-stage methods working on 7 categories	43
3.4	Number of training and test images used for the two-stage methods working on 6 categories	44
3.5	Number of training and test images used for the two-stage methods working on 5 categories	45
3.6	Number of training and test images used for the two-stage methods working on 4 categories	46

3.7	Number of training and test images used for the two-stage methods working on 3 categories	47
3.8	Number of training and test images used for the two-stage methods working on 2 categories	48
3.9	The total target detection accuracies and false alarm rates ob- tained with various numbers of training images on 10 categories .	51
3.10	Number of training and test images used for the two-stage methods working on 10 categories of the new database	52

To my family . . .

Chapter 1

Introduction

Synthetic Aperture Radar (SAR) sensors can produce images of scenes in all weather conditions at any time of day and night which is not possible with infrared or optical sensors. Another useful feature of SARs is the geometric resolution that does not depend upon the operating frequency. Because of these reasons, automatic recognition and classification of man-made (metal) objects in SAR images have been an active research area in recent years [1, 2]. There are many application areas in which the recognition of a target or texture signal is important in SAR images. Besides target detection and classification for military purposes, applications of SAR include recognition of the terrain surface for mineral exploration, determining the spilled oil boundaries in oceans for environmentalists and extracting the sea state and ice hazard maps for navigators. Furthermore, the number of applications can be increased in other areas including military combat identification, meteorological observation, battlefield surveillance, mining, oceanography, classification of earth terrain etc. [2].

SAR images are typically two dimensional (2-D) images. A SAR image perpendicular to the aircraft's direction is constructed as in the following Fig. 1.1 adopted from [3]. The first dimension is called range (or cross track), which is

a measure for the line-of-sight distance of the target to the aircraft. Similar to most radars, the range is determined by measuring the time between the transmitted pulse and its echo. A narrow pulse width leads to a high resolution in range. The other dimension is named as azimuth, which is along the track of the aircraft. To have fine azimuth resolution, a physically large antenna is needed, which is impossible to be deployed on an aircraft. Instead, to produce the data of a large antenna, pieces of data are collected and processed as the aircraft flies along its track in a certain distance called synthetic aperture distance.

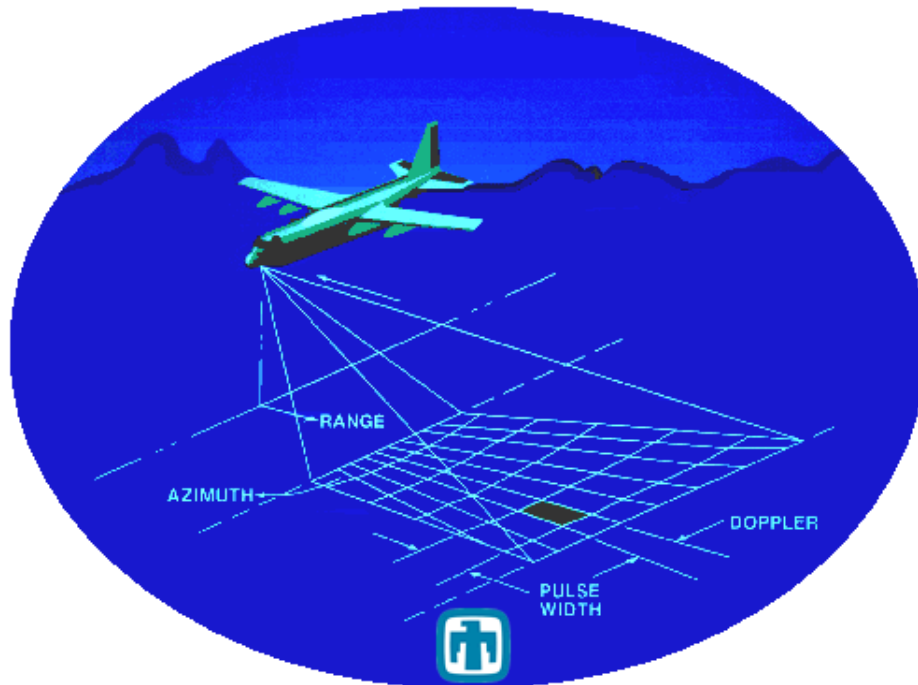


Figure 1.1: Synthetic aperture radar (SAR) working principle (adopted from [3]).

There are numerous advantages of the SAR system as described above. These advantages make target detection and classification in SAR images specifically vital. Many SAR Automatic Target Recognition (ATR) algorithms were developed in the literature [6] -[11]. As shown in Fig. 1.2, a complete ATR system includes five stages: detection, discrimination, classification, recognition, and identification. In many systems, only some of the above stages are available. Therefore,



Figure 1.2: Block diagram of a typical SAR ATR (Automatic Target Recognition) system.

a typical SAR ATR system fulfils three functions: detection (pre-screener), discrimination and classification as will be discussed in Chapter 2. The contribution of this thesis is in the area of detection (pre-screener) or discrimination stage of the SAR ATR.

1.2 Feature extraction from SAR images

Porikli and Tuzel used the region covariance (RC) method to describe an image region using the covariance matrix in order to extract features for detection and classification problems. The RC approach provides robustness on the images in terms of orientation and illumination changes to a certain degree. Moreover, the dimensionality of the covariance matrix does not change with the size of the input image region. In recent years, region covariance is successfully used in face, human, license plate, various objects and texture detection and classification problems in still images and video [12, 13, 14, 15].

In this thesis, the RC and the codifference matrix methods are used in SAR ATR target detection problem. Feature parameters of the region of interests (ROIs) in the images are extracted using the RC method proposed by Porikli et al. The goal is to describe an image region with a covariance matrix for detection of man-made objects in SAR images. The computational cost of the RC method is reduced by introducing a new matrix called codifference matrix which can be used instead of the RC matrix. Various distance metrics are introduced along with the one used in [12] to match the closest regions within the search space of

images. Support Vector Machines (SVMs), which implement Euclidean distance as parameter of measure, are also used as a part of the decision strategy. In real-time applications, SVM classifiers provide the least computational complexity. Simulation results are presented by comparing the proposed approaches to a former method using Principal Component Analysis (PCA) with SVM.

In our work, SAR images are pre-processed with directional filters before the RC and the codifference algorithm. This approach makes it possible to classify ROIs in the training stage into various categories, which results in a reduction on the number of training images to be compared. Therefore, the computational cost of the algorithm significantly decreases as distances between test and the training feature vectors are determined by one-to-one matching between these vectors through l_1 norms. Same principle is not valid for the decisions made with SVM, as total number of images trained stays equal with the old methods. Still the results obtained by SVMs are presented for comparing SVMs' detection performances to the methods using l_1 norm based distance metric.

All simulations are carried out using the images of the MSTAR (Moving and Stationary Target Recognition) SAR database [16], which is the only publicly available database. The database includes the images of various types of fields and targets which include armed personal carriers and a tank made by the Former Soviet Union. Simulation results are presented at the end of each chapter.

1.3 Thesis Outline

The rest of this thesis is organized as follows. In Chapter 2, the RC and region codifference target detection methods are stated and simulation results with different distance measures are given with comparisons to SVM and PCA methods. Chapter 3 introduces the use of directional filters as a pre-processor to the RC and region codifference method with simulation results on decisions made using

l_1 norm distance metric and SVM classifiers. Conclusions are made and a list of future research areas is given in Chapter 4.

Chapter 2

Target Detection in SAR Images Using Region Covariance (RC) and Codifference

In this chapter, the use of region covariance (RC) and codifference matrices in order to detect targets in SAR (Synthetic Aperture Radar) images is described. These matrices form the features of the region of interests (ROIs) extracted from the target and clutter images. Distances between the features of test and training images are calculated with different metrics to be introduced. In addition, SVMs (Support Vector Machines) are used to detect targets in the SAR images.

The images used in this thesis are obtained from the only publicly available SAR database: MSTAR (Moving and Stationary Target Recognition) database [16]. The contents of this database can be found in Section 2.4. The images are divided into training and test datasets. The test image features are matched to target or clutter train image features using different distance metrics based on generalized or distinct eigenvalues and l_1 norms with and without various normalizations. $K - NN$ (k-Nearest Neighbor) algorithm is also tried on

the decisions made with l_1 norm distance metric. Furthermore, SVMs are used to train and test the covariance and codifference features. Simulation results are compared with a PCA (Principal Component Analysis) based method which is also using SVM. The results include target detection accuracies and false alarm (incorrectly classified clutter images) rates. Simulations to obtain the results were carried out using a *MATLAB* computing environment (version R2009b).

The region covariance method was first introduced by Porikli et al. The related work on this method is briefly discussed in Section 2.1. The codifference matrix, developed over the course of this thesis, is defined by modifying the RC matrix and has lower computational cost.

The RC and codifference approach investigated in this chapter can be used in the detection and discrimination stages of a SAR ATR system. Target detection and discrimination are the first stages of a typical SAR ATR system. These stages are important in improving the whole ATR system's performance. In Fig. 2.1 adopted from the works of Novak et al. [4], one can see both target detection and discrimination process forming the first two stages of the three-stage baseline SAR ATR system. Images without potential targets and natural clutter false alarms are rejected in these stages. There are many target detection and discrimination algorithms for SAR images described in the literature [6] - [10]. CFAR (constant false alarm rate) method is generally used for target detection. It uses the amplitude information and discards the phase of the SAR images, which involves excess data [4, 5, 17].

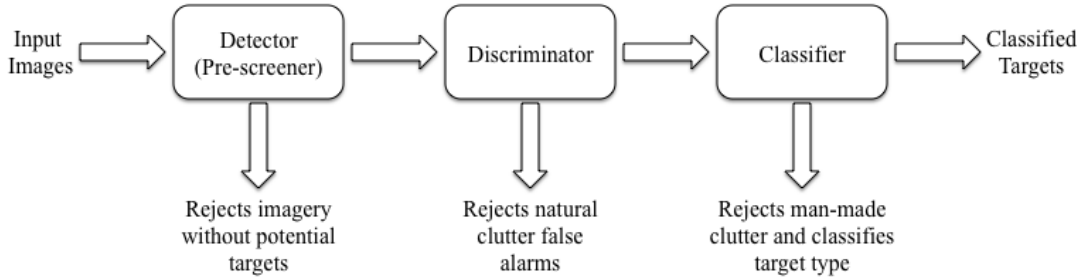


Figure 2.1: Block diagram of three-stage baseline SAR ATR system proposed by Novak et al. [4].

The remaining parts of this chapter are organized as follows. The related work in literature on Porikli’s RC method is presented in Section 2.1. RC and codifference matrices are presented in detail in Sections 2.2 and 2.3. The MSTAR database is overviewed in Section 2.4 and the target detection stages are revealed in Section 2.5. Finally, simulation results on the MSTAR SAR database are delivered in Section 2.6.

2.1 Related Work on Region Covariance (RC) Method

The region covariance (RC) method describes an image region with a covariance matrix in order to extract features for image detection and classification problems. In recent years, this method is successfully used in face, human, license plate and different objects detection and classification problems [12, 13, 14].

Given a ROI where the object to be detected is searched, one or more covariance matrices are computed for cropped chips of the ROI in different size. The covariance features are fed to a multi-layer neural network [14] or Logit-Boost classifiers [13]. Besides learning mechanisms, a distance metric involving

computation of generalized eigenvalues is used in order to match the covariance descriptors [12]. The RC method is also adapted to object tracking applications in video, where the object is described using the covariance matrix [15]. In a frame, the object is found in the ROI where the minimum distance between the RC matrix of the model object and the ROI is achieved. From frame to frame, the variations are adapted by keeping a set of previous RC matrices and extracting a mean on the Riemannian manifolds. The system is shown to be accurately detecting non-rigid, moving objects in non-stationary camera sequences while achieving a detection rate of 97.4% in [15].

In this work, the RC method is applied to SAR images to detect man-made (metal) objects. The distance metric based on the generalized eigenvalues in [12] is used besides other metrics in matching the matrix features extracted from the training and test images.

2.2 Region Covariance (RC) Matrix

In this section, the region covariance (RC) as an image region descriptor is presented. In ROIs of the target and clutter images in the MSTAR database, RC matrix is used to extract feature parameters.

To detect targets on SAR images, one RC matrix is extracted for a ROI. It is assumed that features obtained from a single covariance matrix are enough to discriminate between distributions, which results in minimum computational cost for the algorithm. For each pixel in the ROI, a seven-dimensional feature vector z is computed as,

$$z_k = \left[x \quad y \quad I(x, y) \quad \frac{dI(x,y)}{dx} \quad \frac{dI(x,y)}{dy} \quad \frac{d^2I(x,y)}{dx^2} \quad \frac{d^2I(x,y)}{dy^2} \right] \quad (2.1)$$

where, k is the label of a pixel, (x, y) is the position of a pixel, I is intensity of a pixel (as gray scale images are used in this work), $dI(x, y)/dx$ is the horizontal

and $dI(x, y)/dy$ is the vertical derivative of the ROI calculated through the filter $[-1 \ 0 \ 1]$, $d^2I(x, y)/dx^2$ is the horizontal and $d^2I(x, y)/dy^2$ is the vertical second derivative of the ROI calculated through the filter $[-1 \ 2 \ -1]$. For a 4 by 4 region, $k = 1, 2, \dots, 16$; $x = -2, 1, 0, 1$. One should note that in filtering processes, there is no need for computationally costly multiplications, as the result can be found out by addition and subtraction of the shifted sequences of input data.

Different items could be added to the feature vector z as in [13]. Again, let the feature vector z be defined as:

$$z_k = [z_k(i)]^T \quad (2.2)$$

where i is the index of the feature vector. After obtaining this vector, a fast method for computing the RC matrices by using integral images is applied. This method has the same calculation complexity for all window sizes after computing the integral images as provided in [18]. The 7-by-7 covariance matrix C_R of a ROI R is defined by the fast covariance matrix computation formula:

$$C_R = [c_R(i, j)] = \left(\frac{1}{n-1} \left[\sum_{k=1}^n (z_k(i)z_k(j)) - \frac{1}{n} \sum_{k=1}^n z_k(i) \sum_{k=1}^n z_k(j) \right] \right) \quad (2.3)$$

where n is the total number of pixels in the ROI and $c_R(i, j)$ is the $(i, j)^{th}$ component of the covariance matrix.

There are several advantages of using covariance features to describe a ROI. First, these features have small dimension and they are invariant to a degree of scale and illumination change as these characteristics are all absorbed within the covariance matrix. For instance, given a ROI, its covariance C_R does not have any information regarding the number of pixels, because size of the C_R is due to the number of items in feature vector z , not to the number of pixels in the ROI. By providing C_R as a feature, we look to the relations between the pixels, which absorb certain illumination changes from image to image. In addition, the computation of covariance intrinsically provides an averaging filter to filter out the natural occurring speckle noise that corrupts SAR images.

2.3 Region Codifference Matrix

In this section, a new region codifference matrix is introduced for target detection which replaces the covariance matrix in the novel RC method.

Computational cost of a single covariance matrix is not heavy. However, computational cost becomes important when scanning large regions at different scales and locations. Furthermore, many video processing applications require real-time solutions. In order to decrease the computational cost, the RC matrix definition in Eq. 2.3 is modified to obtain the codifference equation as in Eq. 2.4.

$$C_R = [c_R(i, j)] = \left(\frac{1}{n-1} \left[\sum_{k=1}^n (z_k(i) \oplus z_k(j)) - \frac{1}{n} \sum_{k=1}^n z_k(i) \oplus \sum_{k=1}^n z_k(j) \right] \right) \quad (2.4)$$

where the scalar multiplication is replaced by an additive operator \oplus . The operator \oplus is basically a summation operation but the sign of the results behaves similar to the multiplication operation.

$$a \oplus b = \begin{cases} a + b & \text{if } a \geq 0 \text{ and } b \geq 0 \\ a - b & \text{if } a \leq 0 \text{ and } b \geq 0 \\ -a + b & \text{if } a \geq 0 \text{ and } b \leq 0 \\ -a - b & \text{if } a \leq 0 \text{ and } b \leq 0 \end{cases} \quad (2.5)$$

for real numbers a and b . Above equation can be expressed also as follows:

$$a \oplus b = \text{sign}(a \times b)(|a| + |b|) \quad (2.6)$$

Since $a \oplus b = b \oplus a$, the codifference matrix is also symmetric like the RC matrix. The codifference matrix behaves similar to the covariance matrix. For two variables, the sign of the result for the operations in covariance and codifference is the same. If two variables' signs are the same, the output is positive and if they are not, the output is negative. In many computer systems, addition is less costly compared to multiplication. This makes the calculation of the codifference matrix computationally efficient compared to the covariance matrix.

The operator \oplus satisfies totality, associativity and identity properties; therefore it is a monoid function. In other words it is a semigroup with identity property. Similar statistical methods are used in [19]. Another similar statistical function is the Average Magnitude Difference Function (AMDF), which is widely used in speech processing to determine periodicity of voiced sounds.

2.4 The Moving and Stationary Target Recognition SAR Database

The MSTAR (Moving and Stationary Target Recognition) data was collected using the Sandia National Laboratories Twin Otter SAR sensor payload operating at X band (10 GHz). DHC-6 Twin Otter Aircraft which carries this SAR sensor is shown in Fig. 2.2 [3]. This data was collected and distributed under the DARPA (Defense Advanced Research Projects Agency) MSTAR program. One of the full size X band SAR image collected in this program is shown in Fig. 2.3. The images have 0.3m x 0.3m resolution. All SAR images are acquired at angle of depressions of 15° and 17° . Besides, target images are available in all orientations in the database, i.e. the shots are made over 360° target aspect. In this thesis, all images are treated in an equal manner and all target and clutter images are divided into training and test datasets.



Figure 2.2: DHC-6 Twin Otter Aircraft which carries Sandia National Laboratories Twin Otter SAR sensor (adopted from [3]).

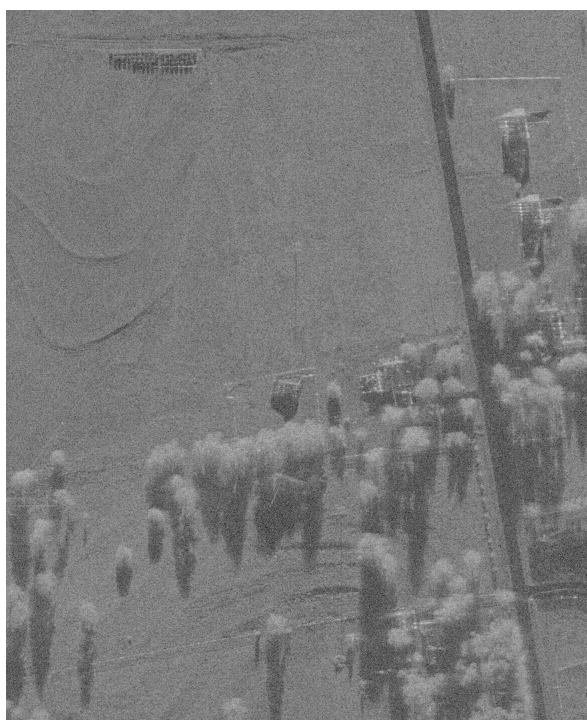


Figure 2.3: A sample for X band SAR image collected in DARPA Moving and Stationary Target Recognition (MSTAR) program.

MSTAR SAR database used in this thesis is the only publicly available database for SAR imagery. However, obtaining the database still requires a formal registration. The database includes images of targets and clutter. Target images consist of the images of armored personnel carriers BMP-2, BTR-70 and T-72 main battle tank of Former Soviet Union. Images of open fields, farms,

trees, roads and buildings form the clutter images. Therefore there is natural and also cultural clutter in the images. The database contains images of three different vehicles for BMP-2 and T-72, however one for BTR-70. The pictures of these vehicles adopted from [5] are presented in Fig. 2.4. Several target and clutter SAR images in the MSTAR database are provided in Fig. 2.5. A total of 1285 BMP-2, 429 BTR-70 and 1045 T-72 images are available in the database. The target images are originally provided in 128-by-128 pixel size chips. The clutter images are cropped in this size randomly from the original 1476-by-1784 sized images (one is shown in Fig. 2.3).

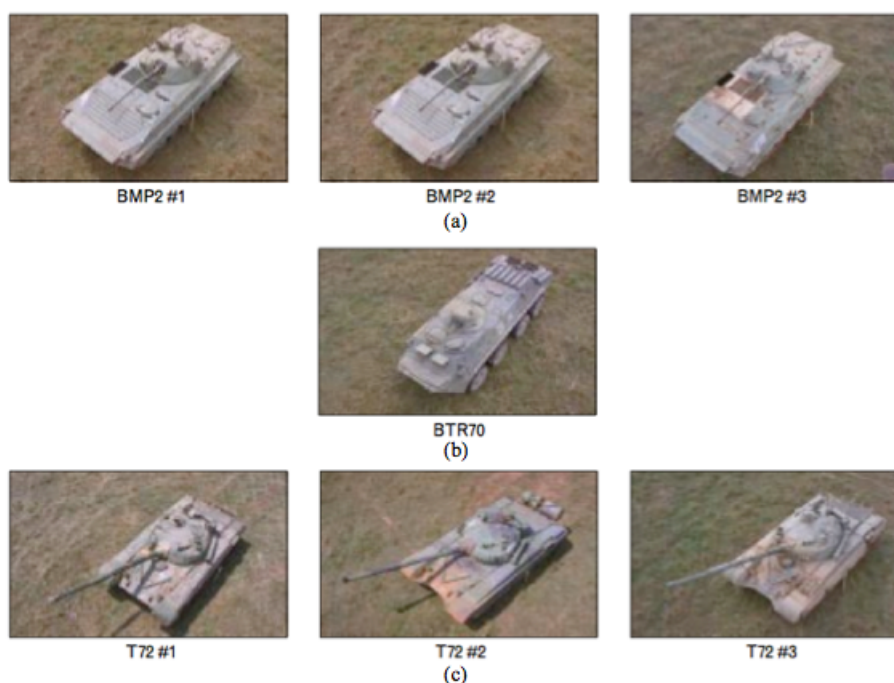


Figure 2.4: Targets in the MSTAR: (a) BMP-2 Armored Personal Carrier, (b) BTR-70 Armored Personal Carrier, (c) T-72 Main Battle Tank [5].

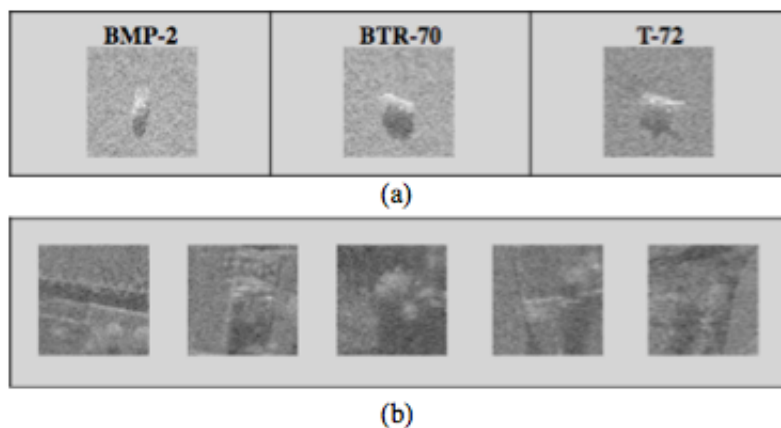


Figure 2.5: Several target and clutter images: (a) Target images of size 128-by-128, (b) Clutter images of size 128-by-128.

2.5 Stages of the Target Detection Algorithm

As mentioned earlier, to detect a target, covariance and codifference matrices of target/clutter training and test images are compared to each other using distance metrics providing robust detection and classification. The block diagram of the entire target detection process is illustrated in Fig. 2.6. First, the ROIs of the images in the database (shown in Fig. 2.8) are divided in two datasets as training and test images. Then, as given in Eq. 2.1, the feature vectors of these images are computed for each pixel. The covariance or codifference matrix of the ROIs using these feature vectors is extracted according to Equations 2.3 and 2.4. The distance between the training and test images are found using various distance metrics on vectors of covariance and codifference features. The label (target/clutter) of training image's ROI producing the smallest distance value determines whether a test image is classified as target or clutter. Thus, target and clutter images of the test dataset are predicted by this way. The covariance and codifference features of training images are also put into SVMs (Support

Vector Machines) and the SVM classifiers are used as a last stage for the target detection algorithm. The results are presented in Section 2.6.1.

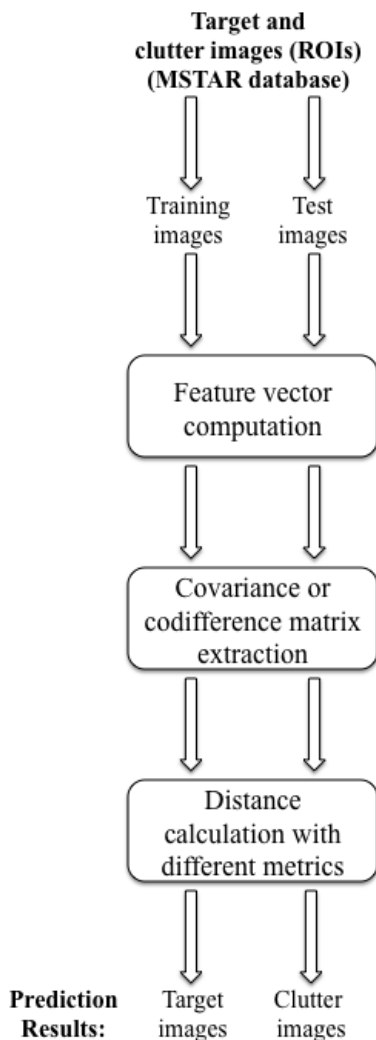


Figure 2.6: Block diagram showing stages of the target detection algorithm.

There is no need to use the entire covariance or codifference matrix as input parameters (features) to the decision mechanism. Let the matrix C_R in Fig. 2.7 illustrate a covariance or a codifference matrix of a ROI. This matrix is symmetric, and therefore the lower (or upper) triangle of the matrix carries the sufficient information for the entire matrix. Moreover, $c_R(1, 1)$, $c_R(2, 1)$ and $c_R(2, 2)$ are eliminated as these are computed from the (x, y) positions in the feature vector z and are equal in every covariance and codifference matrices, as only one matrix

is extracted from each image. As a result, the necessary covariance or codifference features shrink only to the bounded components providing a decrease in computational cost of the decision stage.

$$C_R = \begin{bmatrix} c_R(1,1) & c_R(1,2) & c_R(1,3) & c_R(1,4) & c_R(1,5) & c_R(1,6) & c_R(1,7) \\ c_R(2,1) & c_R(2,2) & c_R(2,3) & c_R(2,4) & c_R(2,5) & c_R(2,6) & c_R(2,7) \\ c_R(3,1) & c_R(3,2) & c_R(3,3) & c_R(3,4) & c_R(3,5) & c_R(3,6) & c_R(3,7) \\ c_R(4,1) & c_R(4,2) & c_R(4,3) & c_R(4,4) & c_R(4,5) & c_R(4,6) & c_R(4,7) \\ c_R(5,1) & c_R(5,2) & c_R(5,3) & c_R(5,4) & c_R(5,5) & c_R(5,6) & c_R(5,7) \\ c_R(6,1) & c_R(6,2) & c_R(6,3) & c_R(6,4) & c_R(6,5) & c_R(6,6) & c_R(6,7) \\ c_R(7,1) & c_R(7,2) & c_R(7,3) & c_R(7,4) & c_R(7,5) & c_R(7,6) & c_R(7,7) \end{bmatrix}$$

Figure 2.7: A sample covariance or codifference matrix where the bounded region shows the necessary features for the decision algorithm.

The original target and cropped clutter images of size 128-by-128 pixels and 64-by-64 image chips cut from the original images form the ROIs. The cropped image chips are chosen by inspection, such that the targets are captured as demonstrated in Fig. 2.8. If the original image is depicted by I , $I(45 : 108, 33 : 96)$ represent the 64-by-64 image chip cropped. These chips provide data size reduction during the feature extraction phase, where horizontal and vertical filtering is used.

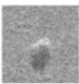
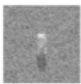
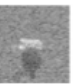
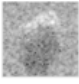
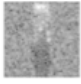
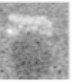

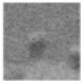
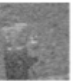

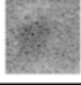

	Targets		
Image Size	BMP-2	BTR-70	T-72
128-by-128			
64-by-64 (Zoomed)			
	Clutter		
128-by-128			
64-by-64 (Zoomed)			

Figure 2.8: Examples of 128-by-128 and 64-by-64 target and clutter images (ROIs). 64-by-64 images are cropped from the 128-by-128 images.

2.6 Simulation Results

Simulation results of the target detection algorithm using RC and codifference methods are presented. In Section 2.6.1, target detection results on covariance and codifference features obtained through various distance metrics and SVM classifiers are delivered. For comparison, SAR image classification results by a former method using PCA (defined in [20]) with SVM are given in Section 2.6.2. The performance of the detection algorithms is determined according to two parameters: (i) detection accuracy = (number of correctly detected target images)/(number of total target test images), (ii) false alarm = (number of clutter images detected as target images)/(number of total clutter test images).

2.6.1 Using Various Distance Metrics and Support Vector Machine (SVM) Classifiers

The number of target and clutter images divided into training and test datasets used in the simulations are presented in Table 2.1. The relation between number of test images and the number of training images is about 20:1, when target images are considered. The ratio rises up to 100:1, when we focus on the clutter images. These high ratios increase the importance of getting accurate target detection and low false alarm rates. Simulation results for whole and target focused 64-by-64 images (ROIs) for the RC and codifference methods using different distance metrics and SVM classifiers are summarized in Tables 2.2, 2.3, 2.4, 2.5, 2.6 and 2.7 in exact ratio and percentages form.

Table 2.1: Number of images used in training and testing studies

	Number of train images	Number of test images
Target	132	2627
Clutter	132	13346

The original distance metric to be used with the RC method is presented by Porikli et. al. [12]. In order to match two ROIs, the calculated covariance matrices are compared to each other using this distance metric based on generalized eigenvalues. Two images (or two ROIs R_1 and R_2) have a distance ρ_1 calculated with their covariance matrices using Eq. 2.7.

$$\rho_1(C_1, C_2) = \sqrt{\sum_{i=1}^p \log^2(\lambda_i(C_1, C_2))} \quad (2.7)$$

Target detection and false alarm rates by using the distance metric in Eq. 2.7 on covariance and codifference matrices are given in Table 2.2.

The studies with the database are expanded such that new distance metrics are defined for comparison of the region covariance and codifference matrices in order to improve the target detection performance. The first modified distance

Table 2.2: Target detection accuracies and false alarm rates achieved using RC and region codifference methods with the distance metric defined in Eq. 2.7

	Input images (ROIs)	Rates	
		Target detection accuracies	False alarm
Using RC method	128-by-128	2625/2627 (99.92%)	86/13346 (0.64%)
	64-by-64	2627/2627 (100%)	1/13346 (~0%)
Using region codifference method	128-by-128	2626/2627 (99.96%)	0/13346 (0%)
	64-by-64	2624/2627 (99.88%)	20/13346 (0.15%)

metric ρ_2 is defined as the square root of the sum of the logarithmic square of the differences between respective eigenvalues of C_1 and C_2 as in Eq. 2.8.

$$\rho_2(C_1, C_2) = \sqrt{\sum_{i=1}^p \log^2(\lambda_i(C_1) - \lambda_i(C_2))} \quad (2.8)$$

where, C_1, C_2 are the covariance matrices of regions R_1 and R_2 , respectively and λ_i is the i^{th} eigenvalue of C_1, C_2 separately and $p(= 7)$ is the number of eigenvalues for C_1 and C_2 . The resulting performance rates using this distance metric are depicted in Table 2.3.

Table 2.3: Target detection accuracies and false alarm rates achieved using RC and region codifference methods with the distance metric defined in Eq. 2.8

	Input images (ROIs)	Rates	
		Target detection accuracies	False alarm
Using RC method	128-by-128	2576/2627 (98.06%)	44/13346 (0.33%)
	64-by-64	2576/2627 (98.06%)	14/13346 (0.1%)
Using region codifference method	128-by-128	2567/2627 (97.72%)	40/13346 (0.3%)
	64-by-64	2575/2627 (98.02%)	66/13346 (0.49%)

A new distance metric is also defined which is based on the l_1 norm distance calculation rather than eigenvalues on two RC or codifference matrices' feature vectors. This distance metric is defined as

$$\rho_3(C_1, C_2) = \sum_{i=1}^p \left[\sum_{j=1}^p (|C_1(i, j) - C_2(i, j)|) \right] \quad (2.9)$$

where, C_1, C_2 are the covariance matrices of regions R_1 and R_2 , respectively. Extracting no eigenvalues and only computing the sum of difference between the training and test covariance and codifference matrix feature vectors significantly reduces the computational cost. The target detection results of SAR images using this distance metric with RC and codifference matrices are shown in Table 2.4.

Table 2.4: Target detection accuracies and false alarm rates achieved using RC and region codifference methods with the distance metric defined in Eq. 2.9

	Input images (ROIs)	Rates	
		Target detection accuracies	False alarm
Using RC method	128-by-128	2618/2627 (99.66%)	0/13346 (0%)
	64-by-64	2626/2627 (99.96%)	1/13346 (~0%)
Using region codifference method	128-by-128	2627/2627 (100%)	0/13346 (0%)
	64-by-64	2626/2627 (99.96%)	1/13346 (~0%)

Further, a new distance metric is introduced which finds distance between two ROIs according to the normalization by the diagonal values of covariance or codifference matrices of only the training regions. Since the pixel intensity values and their derivatives in the feature vector z in Eq. 2.1 have different scales of values, normalization is applied while comparing the covariance and codifference matrices of the two regions computed from them. This metric is given as

$$\rho_4(C_1, C_2) = \sum_{i=1}^p \left[\sum_{j=1}^p \left(\frac{|C_1(i, j) - C_2(i, j)|}{C_2(i, i)} \right) \right] \quad (2.10)$$

where, C_1, C_2 are the covariance matrices of two ROIs R_1 and R_2 , respectively. For this case, R_1 is the region acquired from the test images, whereas R_2 is the region acquired from the training images. The target detection results obtained by applying this distance metric are shown in Table 2.5.

The metric in Eq. 2.10 is also modified such that the normalization is made by contribution of both training and test images' covariance or codifference matrices. This metric is defined as

$$\rho_5(C_1, C_2) = \sum_{i=1}^p \left[\sum_{j=1}^p \left(\frac{|C_1(i, j) - C_2(i, j)|}{(C_1(i, i) + C_2(i, i))} \right) \right] \quad (2.11)$$

Table 2.5: Target detection accuracies and false alarm rates achieved using RC and region codifference methods with the distance metric defined in Eq. 2.10

	Input images (ROIs)	Rates	
		Target detection accuracies	False alarm
Using RC method	128-by-128	2625/2627 (99.92%)	13/13346 (0.10%)
	64-by-64	2627/2627 (100%)	3/13346 (0.02%)
Using region codifference method	128-by-128	2627/2627 (100%)	1/13346 (~0%)
	64-by-64	2626/2627 (99.96%)	0/13346 (0%)

where, C_1 , C_2 are the covariance matrices of regions R_1 (from test images) and R_2 (from training images), respectively. The normalization is done again by the diagonal values of the covariance or codifference matrices. The resulting target detection performances using this metric are given in Table 2.6

Table 2.6: Target detection accuracies and false alarm rates achieved using RC and region codifference methods with the distance metric defined in Eq. 2.11

	Input images (ROIs)	Rates	
		Target detection accuracies	False alarm
Using RC method	128-by-128	2625/2627 (99.92%)	4/13346 (0.03%)
	64-by-64	2627/2627 (100%)	1/13346 (~0%)
Using region codifference method	128-by-128	2626/2627 (99.96%)	0/13346 (0%)
	64-by-64	2626/2627 (99.96%)	0/13346 (0%)

Finally, SVMs are used in order to distinguish between the covariance or codifference feature vectors extracted from the training and test images to detect targets/clutter in the database. SVM is a supervised machine learning method based on the statistical learning theory and approach developed by Vladimir Vapnik. SVMs have been applied to SAR target classification problems and they exhibit superior performance measures compared to other classifiers [9]. There are many parameters corresponding to different SVM kernels. In this study, the polynomial SVM kernel proposed in [21] is chosen, although, the RBF (Radial Basis Function) and linear SVM kernels are also implemented. It is observed

that when RBF kernel is used on the RC features, it fails to classify almost half of the target and clutter test images into any decision group. This kernel also returns high false alarm rates, when it is used with the region codifference method. Therefore, the RBF kernel does not provide any good results unlike the polynomial kernel. The overall classification performance also decreases when linear kernel is used. As a result, among the three kernels, the polynomial kernel gives the best performance rate for the SAR target detection problem investigated in this thesis. Thus, the results acquired through SVM with polynomial kernel are given in Table 2.7

Table 2.7: Target detection accuracies and false alarm rates achieved using SVM as a classifier

	Input images (ROIs)	Rates	
		Target detection accuracies	False alarm
Using RC method	128-by-128	2622/2627 (99.81%)	6/13346 (0.04%)
	64-by-64	2617/2627 (99.62%)	6/13346 (0.04%)
Using region codifference method	128-by-128	2627/2627 (100%)	0/13346 (0%)
	64-by-64	2626/2627 (99.96%)	1/13346 (~0%)

The tables in this section showing the results obtained from the presented methods are summarized in Figures 2.9 and 2.10.

First of all, it is observed that Porikli's distance metric provides a good target detection performance, however it suffers from high false alarm rates. Computing the sum of the logarithmic square differences between the eigenvalues of the matrices as in Eq. 2.8 produces worse classification results than Porikli's distance metric in Eq. 2.7. Tables and figures indicate that the highest detection accuracy with the lowest false alarm rate is achieved when l_1 norm distance based metric is used with codifference method for SAR target and clutter image classification. Hence, for 64-by-64 images, the l_1 norm distance metric produces the highest detection accuracy and lowest false alarm rate. This is the reason for using this

distance metric in Chapter 3. Furthermore, it has the lowest computational cost compared to other distance measures.

SVM classifiers work also well with codifference matrix features and they provide about 100% target detection rates likewise the distance metrics based on l_1 norms. Same argument is not true when RC matrix feature vectors are used as input into SVM classifiers. However, for real-time applications, testing images using SVMs provides the lowest computational complexity.

Finally, the studies show that in most cases region codifference features are describing the ROIs that they represent better than the RC features. Thus, the target detection and false alarm performances are generally better when codifference matrices are used. The reader should recall that another advantage of using codifference matrices is the lower computational cost that they bring to the overall image classification system, as described in Section 2.3.

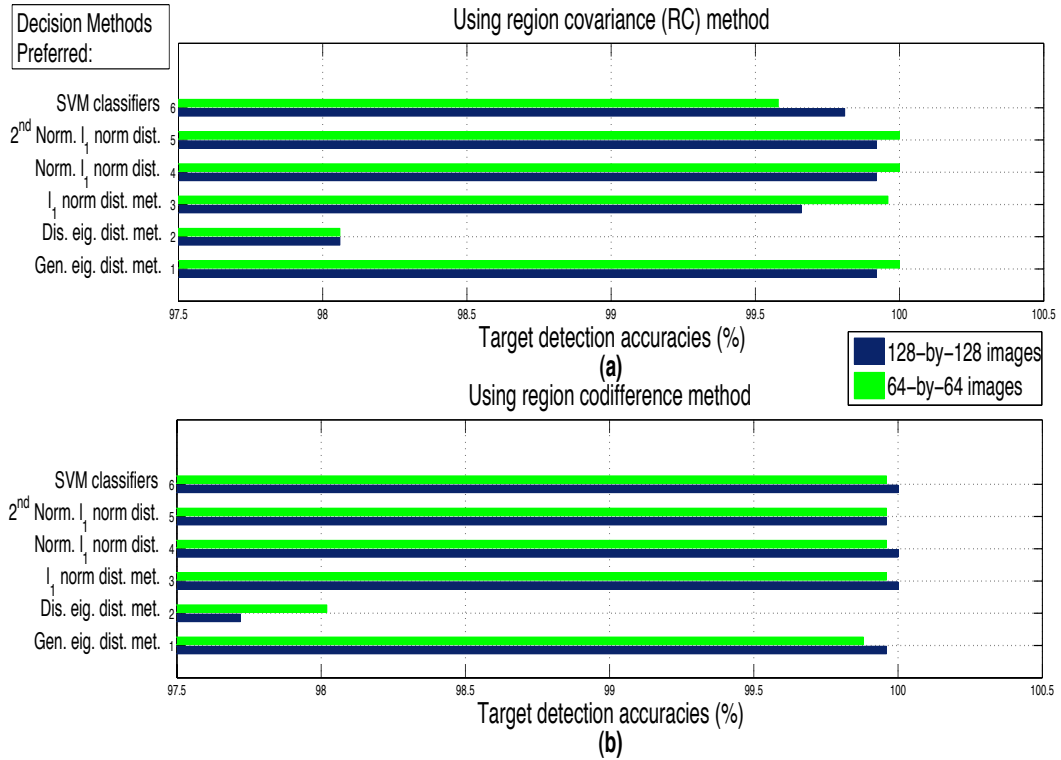


Figure 2.9: The target detection accuracies (%) obtained with various decision techniques using (a) RC and (b) codifference methods proposed.

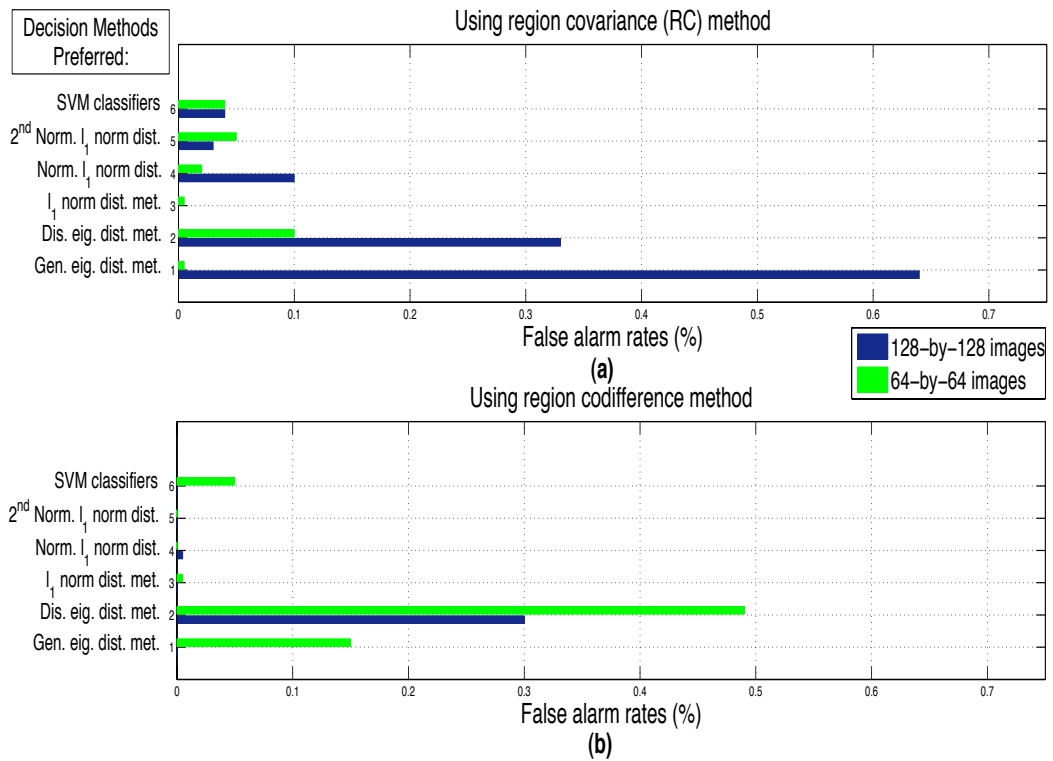


Figure 2.10: The false alarm rates (%) obtained with various decision techniques using (a) RC and (b) codifference methods proposed.

The results upto this point are obtained with 132 target and clutter training images. In Table 2.8, one can see the target detection accuracies and false alarm rates acquired using RC and codifference methods with l_1 norm distance metric and SVM classifiers after increasing or decreasing the number of target and clutter training images. As the number of training images increases, the target detection accuracies also increase. However, the behaviour of false alarm rates are unpredictable.

Table 2.8: The target detection accuracies and false alarm rates obtained with various numbers of training images

Number of training images				
Target	76	132	174	220
Clutter	76	132	174	220
Simulation results				
Using RC method				
With l_1 norm distance metric				
Target det. accuracies	$\frac{2664}{2683}$ (99.29%)	$\frac{2626}{2627}$ (99.96%)	$\frac{2585}{2585}$ (100%)	$\frac{2539}{2539}$ (100%)
False alarm rates	$\frac{0}{13346}$ (0%)	$\frac{1}{13346}$ ($\sim 0\%$)	$\frac{0}{13346}$ (0%)	$\frac{0}{13346}$ (0%)
With SVM classifiers				
Target det. accuracies	$\frac{2663}{2683}$ (99.25%)	$\frac{2617}{2627}$ (99.62%)	$\frac{2585}{2585}$ (100%)	$\frac{2539}{2539}$ (100%)
False alarm rates	$\frac{0}{13346}$ (0%)	$\frac{6}{13346}$ (0.05%)	$\frac{0}{13346}$ (0%)	$\frac{0}{13346}$ (0%)
Using reg. codifference method				
With l_1 norm distance metric				
Target det. accuracies	$\frac{2675}{2683}$ (99.70%)	$\frac{2626}{2627}$ (99.96%)	$\frac{2585}{2585}$ (100%)	$\frac{2539}{2539}$ (100%)
False alarm rates	$\frac{0}{13346}$ (0%)	$\frac{1}{13346}$ ($\sim 0\%$)	$\frac{0}{13346}$ (0%)	$\frac{3}{13346}$ (0.02%)
With SVM classifiers				
Target det. accuracies	$\frac{2672}{2683}$ (99.59%)	$\frac{2626}{2627}$ (99.96%)	$\frac{2585}{2585}$ (100%)	$\frac{2539}{2539}$ (100%)
False alarm rates	$\frac{0}{13346}$ (0%)	$\frac{1}{13346}$ ($\sim 0\%$)	$\frac{1}{13346}$ ($\sim 0\%$)	$\frac{2}{13346}$ (0.01%)

Using k-Nearest Neighbor (k-NN) Algorithm

K-Nearest Neighbor ($k-NN$) algorithm is a method for classifying objects based on the closest training samples in the searched feature space. The classification of an object is decided according to the majority vote of its k neighbors in the training dataset. The neighbors stated here are the other objects that have smallest distances with the object to be classified.

The $k - NN$ algorithm is used with the l_1 norm distance metric on RC and codifference methods. The majority of k training images providing smallest l_1 norm distance with the test image assigns whether a test image belongs to a target or clutter. The target detection accuracies and false alarm rates achieved with increasing k values are presented in percentages in the following Figures 2.11 and 2.12.

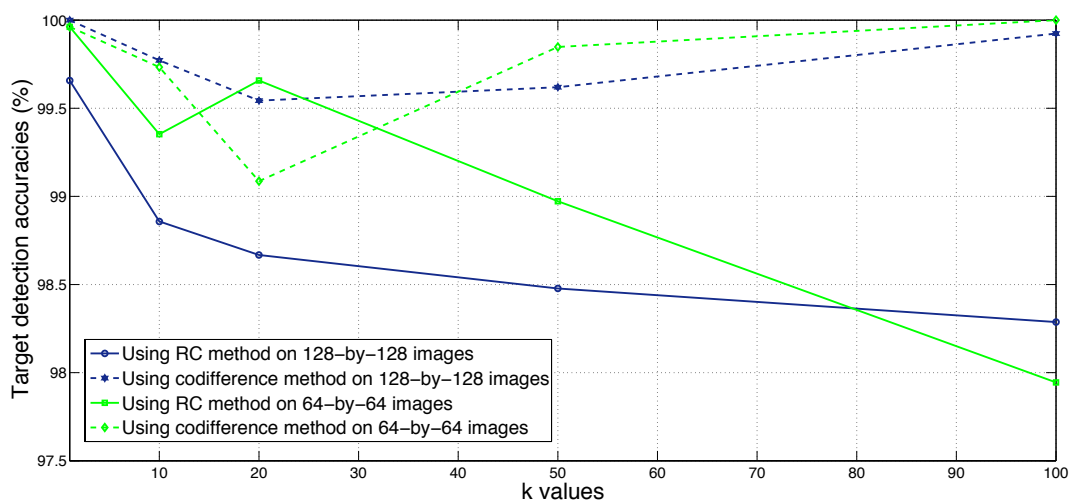


Figure 2.11: The target detection accuracies (%) obtained for increasing k values using l_1 norm distance metric.

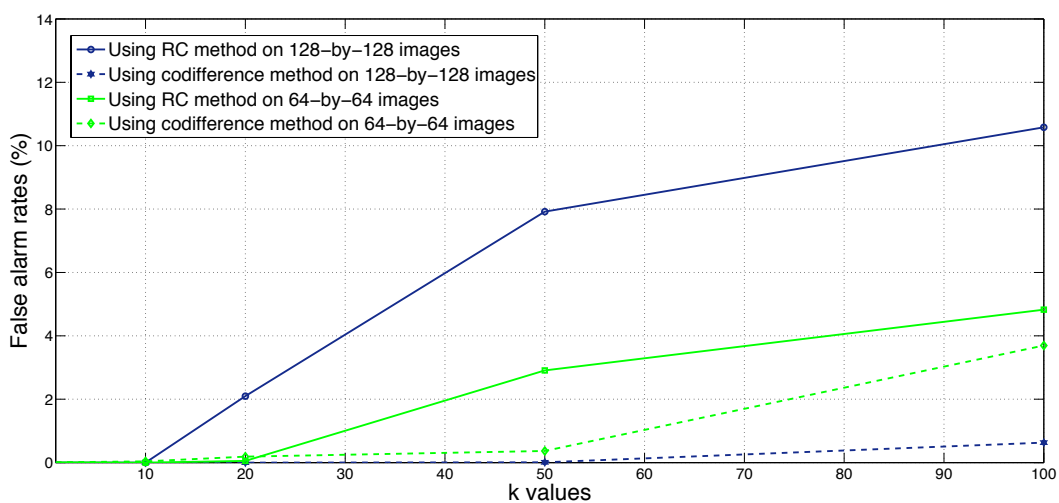


Figure 2.12: The false alarm rates (%) obtained for increasing k values using l_1 norm distance metric.

In Fig. 2.11, it is observed that using RC method leads to lower target detection accuracies with increasing k values. When region codifference method is considered, the target detection accuracies drop until $k = 20$, but rise again until the largest k value.

The false alarm rates increase gradually for both the RC and codifference methods, when k is increased. However, the rise is huge when RC matrices are used to represent the input images.

The responses of the methods presented here to the $k - NN$ algorithm are similar for both 64-by-64 and 128-by-128 sized input SAR images. Commonly, the SAR image classification performance degrades for larger k values. Therefore, the $k - NN$ algorithm brings extra unnecessary computational cost to the system as it does not provide any improvements for the methods presented in this chapter.

2.6.2 Using Principal Component Analysis (PCA) Method

The commonly used Principal Component Analysis (PCA) is applied to the MSTAR database, in order to make comparisons with the presented methods. PCA is basically an eigenvector-based multivariate analysis method which involves extracting a smaller number of uncorrelated variables named principal components from a number of possibly correlated variables [20]. This method is widely applied in many types of analysis such as neuroscience, face recognition, image compression due to its simple, non-parametric nature and ability to reduce data of high dimensionality to lower dimensionality.

The implementation of PCA includes the following phases: First a dataset is formed from the training images of the database represented by a M by N matrix, where M is the number of samples and N is the vector length, i.e. data dimension of each sample. The mean is subtracted from each data dimension.

The covariance of this new M by N matrix is calculated. Next the eigenvectors and eigenvalues of the covariance matrix are computed. Finally the determined number of principal components is selected to form a feature vector. The number of the principal components, which also corresponds to the length of the feature vector, is important and can be adjusted based on the dataset and performance results. Increasing the number of principal components may degrade the performance. In this work, using more than 8 principal components slightly reduces the target detection and classification performance. The best performance is achieved with 8 principal components. The same polynomial SVM kernel as in Section 2.6.1 is used to train and test these principal components. The numbers of target and clutter images in training and test datasets are given in Table 2.9. The target detection algorithm results using the PCA method are depicted in Table 2.10.

Table 2.9: Number of images used in training and testing studies for the PCA method

	Number of train images	Number of test images
Target	108	2651
Clutter	569	13445

Table 2.10: Target detection accuracies and false alarm rates achieved using PCA method

Input images (ROIs)	Rates	
	Target detection accuracies	False alarm
128-by-128	2644/2651 (99.74%)	0/13445 (0%)
64-by-64	2647/2651 (99.85%)	0/13445 (0%)

The same database used for the PCA method is used on RC and codifference methods presented in this chapter. The decisions are made with l_1 norm distance metric, which is one of the decision methods that gives highest detection performances. Furthermore, this metric provides the lowest computational cost

for the algorithm among other distance measures, as described in Section 2.6.1. The target detection and false alarm rates obtained are presented in Table 2.11.

Table 2.11: Target detection accuracies and false alarm rates achieved using the distance metric defined in Eq. 2.9

	Input images (ROIs)	Rates	
		Target detection accuracies	False alarm
Using RC method	128-by-128	2634/2651 (99.36%)	0/13445 (0%)
	64-by-64	2642/2651 (99.66%)	0/13445 (0%)
Using region codifference method	128-by-128	2649/2651 (99.92%)	0/13445 (0%)
	64-by-64	2648/2651 (99.89%)	0/13445 (0%)

The RC and codifference features are also trained using a SVM classifier on the database used in this section. The prediction results made by the SVM classifier are presented in Table 2.12.

Table 2.12: Target detection accuracies and false alarm rates achieved using SVM as a classifier

	Input images (ROIs)	Rates	
		Target detection accuracies	False alarm
Using RC method	128-by-128	2638/2651 (99.51%)	0/13445 (0%)
	64-by-64	2647/2651 (99.85%)	0/13445 (0%)
Using region codifference method	128-by-128	2649/2651 (99.92%)	0/13445 (0%)
	64-by-64	2648/2651 (99.89%)	0/13445 (0%)

The results in Tables 2.10, 2.11 and 2.12 show that when region codifference matrix features are used with the two decision methods for both 128-by-128 and 64-by-64 sized ROIs, better target detection accuracies are achieved than the PCA method. This is as an expected result as the region codifference method is proven to be generally providing better detection performances than the RC method in the previous sections.

Moreover, it is observed that the false alarm rates acquired from the simulations are always 0%. This is mainly because higher number of clutter training

images is used in the decision process when compared to number of target training images for the simulations implemented in this section.

2.7 Summary

In this chapter, a descriptive feature parameter extraction method from SAR images is proposed. The new approaches are based on RC and region codifference methods. Simulation results of target detection in MSTAR database are presented. The RC method delivers high detection accuracies and low false alarm rates. However, it is observed that the codifference method provides better performance than the RC method and PCA method with accurate SAR image classification performances. Furthermore, simulation results indicate that the best detection and false alarm rates are achieved when the l_1 norm distance metric is used to match two codifference matrix feature vectors instead of measures involving computation of eigenvalues or using SVM classifiers. The work presented in this chapter is published in [22].

Chapter 3

Use of Directional Filters (DFs) on Target Detection Methods

3.1 Introduction

Target detection in SAR images using region covariance (RC) and codifference methods is shown to be accurate in Chapter 2 despite the high computational cost. The proposed method in this chapter uses directional filters in order to decrease the search space. As a result the computational cost of the RC and codifference based algorithm significantly falls as the number of comparisons decrease. Images in MSTAR SAR database are first classified into several categories using directional filters (DFs). Target and clutter image features are extracted using RC and codifference methods in each category. Features of the test dataset are compared to a lower number of features in the training dataset using l_1 norm distance metric in Eq. 2.9. Support Vector Machines (SVMs) which are trained using RC and codifference matrix feature vectors are also used in decision making within each category. Simulation results are presented.

In this chapter, a pre-processing stage based on directional filtering is introduced for SAR image classification using the RC and codifference algorithm proposed in the previous chapter. Directional filters were successfully used as a first stage in many applications including vector quantization and image coding [23]-[27]. Regions of interests (ROIs) in SAR images are filtered using two-dimensional directional-wavelet type filters in order to divide both target and clutter images into categories according to their orientations. Then the images are distributed into training and test datasets.

The output of the pre-processing stage is fed to the detection stage in which representative feature parameters are extracted using the covariance and codifference matrices of the ROIs. The distance between matrices is calculated using the l_1 norm distance. The matrices are also used as SVM feature space parameters for discrimination between target and clutter images. Simulations are carried out using a *MATLAB* computing environment (version R2009b). It is observed that the directional approach, when used with l_1 norm distance, reduces the computational complexity without decreasing the target detection accuracy in a significant manner in the MSTAR database. Target detection and false alarm rates are comparable to the methods in Chapter 2 which have higher computational costs. The entire process is illustrated in Fig. 3.1.

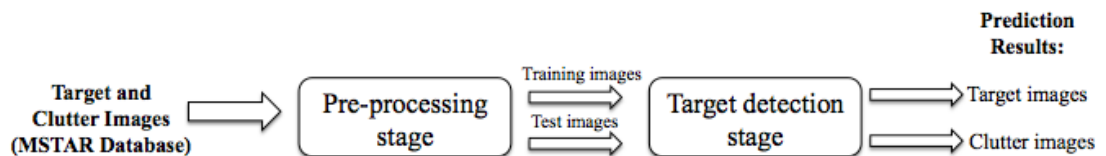


Figure 3.1: Block diagram of the two-stage target detection process investigated in this chapter

The remaining part of this chapter is organised as follows. In Section 3.2, directional filters (DFs) which are used in the pre-processing stage of the algorithm are introduced. The target detection strategy of the two-stage system is described in Section 3.3. Simulation results are presented in Section 3.4 with comparisons of the proposed methods here to the existing methods.

3.2 Pre-processing Stage and Directional Filter (DF) Design

The number of comparisons made in matching with target and clutter images causes a considerable rise in computational cost. The computational cost is mainly due to the straightforward distance computations with high number of training samples. This cost has to be reduced when one wants to scan large image regions at different locations. In addition, the target detection algorithm is also expected to be used in real-time applications. In this section, a pre-processing stage is proposed which consists of applying directional filters (DFs) to classify target and clutter images to categories according to their orientations. As the nature of this process suggests, smaller number of images are used within categories in decision of target or clutter images, and therefore computational cost of the target detection algorithm decreases significantly with the proposed pre-processing stage.

The design principle of the DFs used in this work is illustrated in Fig. 3.2. On the left hand side, 7-by-7 horizontal DF is shown. This filter is used as the template filter to design the other DFs. Along the horizontal axis, the filter coefficient values change from -1 to 1 in 7 steps in a linear manner. The other directional filters are produced from the template filter coefficient matrix by rotation. To obtain the first filter DF1 from the template DF, the outermost pixels are rotated clockwise by one unit as shown in Fig. 3.2. The second filter DF2 is

obtained from DF1 in a similar manner. In DF2, the inner filter coefficients are also rotated clockwise by one step. The DF3 is obtained from the DF2, and it is a diagonal filter. The DF4 and the DF5 are 90° rotated versions of DF1 and DF2, respectively. Filters DF6-DF10 are symmetric with respect to DF1-DF5 on vertical axis, respectively. All the DFs are shown in Fig. 3.2. Samples of obtained target images can also be seen in Fig. 3.5.

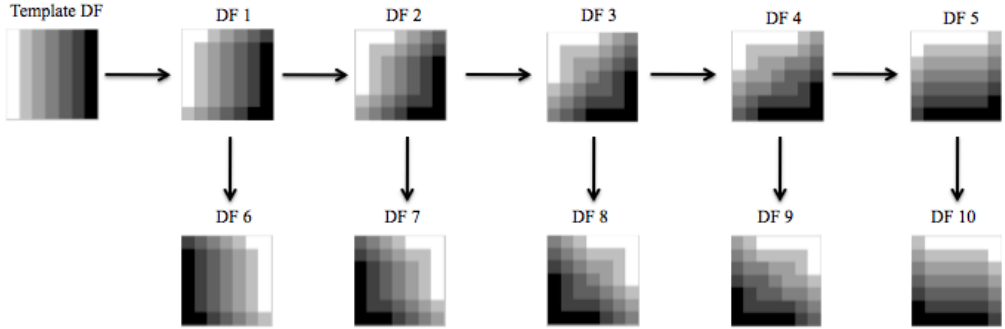


Figure 3.2: Design of the directional filters (DFs)

As it can also be observed from the sample target and clutter images in Figures 2.5 and 2.8, the objects in SAR images are brighter to the top of them, providing natural vertical edges for all the ROIs. This property of the SAR images provides the images to be accurately classified into categories, as DF1-DF10 are designed to pick up the images having vertical edges between -90° and 90° rotation in 10 steps. However, a sharp vertical filter is avoided, because it tends to bring up more images to its category than the other filters. Similarly, a sharp horizontal filter (see template filter in Fig. 3.2) tends to bring less number of images to its category compared to DF1-DF10.

In Fig. 3.3, the block diagram of the pre-processing stage is presented. First, the original 128-by-128 input target images obtained from the MSTAR database are cropped such that the targets and their shades are covered in the new 64-by-64 images, as described in Section 2.5. These 64-by-64 images are chosen simply because processing them is less costly and the studies in Chapter 2 show that they

give close detection performances to the 128-by-128 images. Then, these cropped images are decimated by a factor of two in each dimension before applying the directional filters in order to match the DF size with the targets. To prevent aliasing a simple 3-by-3 low-pass Gaussian filter is used during decimation. The coefficients of this filter, H_{LPF} is as follows,

$$H_{LPF} = \begin{bmatrix} \frac{1}{16} & \frac{1}{8} & \frac{1}{16} \\ \frac{1}{8} & \frac{1}{4} & \frac{1}{8} \\ \frac{1}{16} & \frac{1}{8} & \frac{1}{16} \end{bmatrix}$$

After applying DFs, the l_1 norm of the output images are calculated as $M_R = ||R(x, y)||_1$, where M_R represents the magnitude of the image region R . Finally, the cropped images are categorized under the number of the filter that they give the highest norm. As a result, the n^{th} category contains the 64-by-64 target images that produces the highest l_1 energy output to DF n . Same operations are also applied to 128-by-128 clutter images obtained from the MSTAR database. The cropped 64-by-64 target and clutter images form the ROIs (regions of interests), which are same as the 64-by-64 images used in Chapter 2.

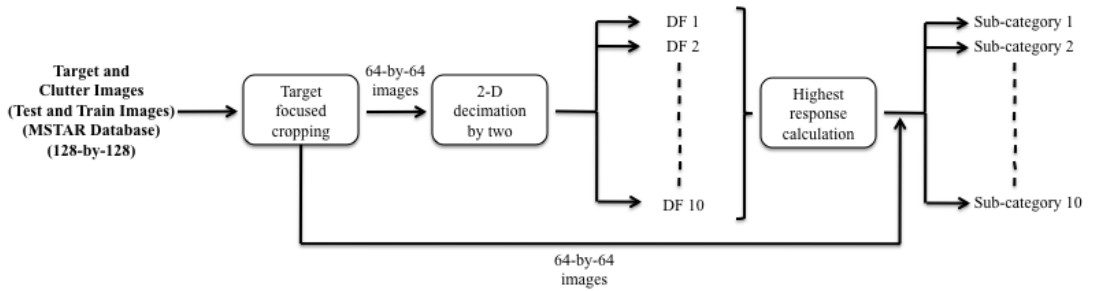


Figure 3.3: Block diagram of the pre-processing stage

Finally, it should be noted that, besides decreasing the computational cost, dividing the SAR images into categories covers up a deficiency in the characteristics of the covariance and codifference matrices. In Sections 2.2 and 2.3, it is

clearly observed that RC and codifference matrix features are not rotationally invariant because the feature vector z that they are built up on also consists of values computed from the first and second derivatives in x (horizontal) and y (vertical) directions. The outputs of directional filters DF1-DF10 provide the objects in the SAR images to be rotationally similar. Therefore a rotational invariance is achieved by applying the pre-processing stage prior to the former target detection algorithm.

3.3 Target Detection Strategy

After distributing the images into categories, training and test datasets are formed from the images. Then, in each category, for each ROIs of the clutter and target images, RC and codifference matrices are extracted as explained in Sections 2.2 and 2.3. 25 bounded coefficients are Fig. 2.7 are sufficient features for target/clutter detection process. Two methods are considered in the decision of whether an image belongs to a target or clutter.

The first method involves distance computation through l_1 norm. The l_1 norms of the differences between the two covariance or codifference matrices' feature vectors are used in decision of whether a test image is a target or clutter image. The l_1 norm distance metric ρ is re-defined in the following equation.

$$\rho(C_1, C_2) = \sum_{i=1}^p \left[\sum_{j=1}^p (|C_1(i, j) - C_2(i, j)|) \right] \quad (3.1)$$

where, C_1, C_2 is the covariance or codifference matrix of ROIs R_1 and R_2 belong to a test and training image in a category and p is the number of items in the feature vector z in Eq. 2.1. There are two reasons why this metric is chosen for target detection simulations presented in this chapter: (i) This metric provides the simplest decision metric among other metrics used in Chapter 2 by calculating only the magnitude of the difference of features. (ii) The metric provides good target detection performance as summarized in Tables 2.4 and 2.11.

For making comparisons with the l_1 norm distance based method, the matrix coefficients from training images are used as feature parameters for training SVM classifiers. This method is also proven earlier to be accurate on target detection with results in Tables 2.7 and 2.12. Besides, SVM classifiers provide the least computational solutions in real-time applications for the SAR image classification problem. The matrix coefficients of test images are compared to the model generated in training phase. The final predictions are obtained according to the classification results of the SVMs which determine whether the input test image is a target image or a clutter image.

The block diagrams of the target detection stage in each category for the considered two methods are shown in Fig. 3.4.

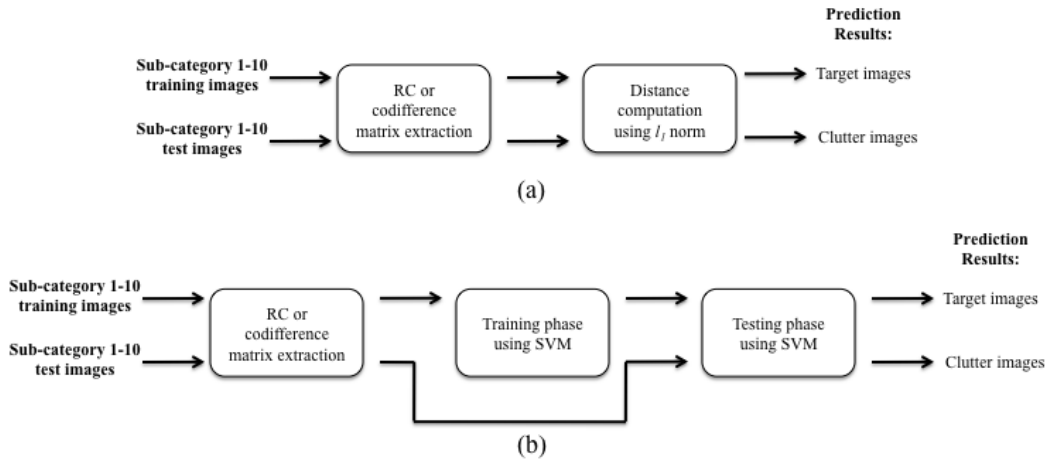


Figure 3.4: Block diagram of the target detection stage applied in each category using (a) l_1 norm distance metric in Eq. 3.1 (b) SVM classifiers.

3.4 Simulation Results

As explained in Sections 3.2 and 3.3, the methods presented here have two stages. Therefore in this section, the proposed algorithm is simply referred as "two-stage"

method. The effect of each stage on the overall target detection performance is illustrated in this section.

As indicated before in Fig. 3.1, the first stage of the algorithm is pre-processing, where target and clutter images belonging to each category are determined using directional filter (DF) outputs. Sample target images belonging to each category are shown in Fig. 3.5. Symbols of DFs are given above the filters. These symbols are used to simplify the tables presented in this section, as they show the orientation of the DFs. As Fig. 3.5 illustrates, the symbols show also the orientation of the targets, which are decided according to the DFs' output that they represent.

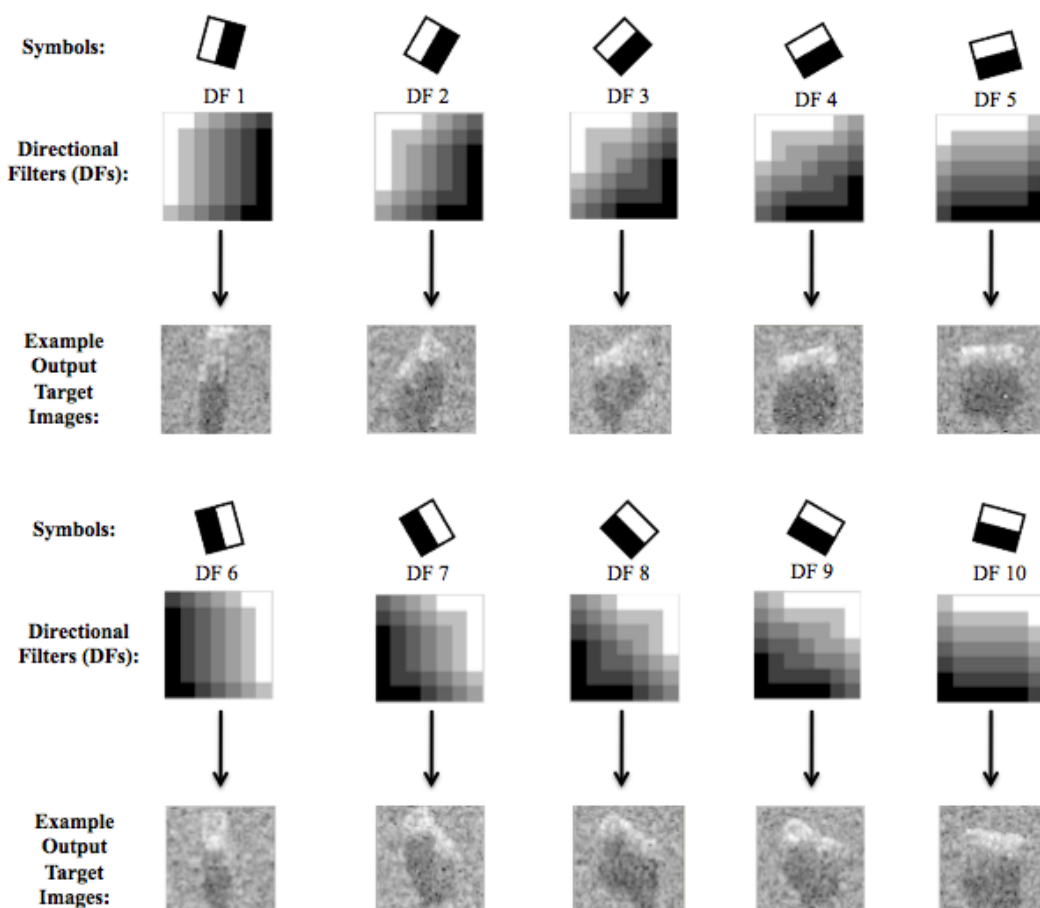












Figure 3.5: Example 64-by-64 target images selected by DFs 1 - 10

The same training and test images as in Section 2.6.1 are used with the methods described in this chapter. The total numbers of target and clutter images divided into training and test datasets are given in Table 2.1. In the first simulation, training and test images are distributed into 10 categories, as mentioned in Section 3.2. Therefore, the number of target and clutter images in the training dataset, decreased to 10-15 in each category from 132 in the older studies (see Table 3.1). Eventually, the number of comparisons made between test and training images with l_1 norm distance metric in Eq. 3.1 are reduced by approximately 90%. This is the main reason for computational efficiency in using the two-stage approach. When the training dataset is put into SVM and models are created for each category, this computational efficiency is no longer available as the total number of images to be trained remains the same with the studies in Chapter 2.

Exact number of target and clutter training and test images at the output of DFs 1-10 is given in Table 3.1. Same numbers of target and clutter images are used in each category. The decisions are made by both using l_1 norm distance metric and SVM classifiers on RC and codifference features. Simulation results are summarized in Fig. 3.6, which includes target detection accuracies and false alarm (incorrectly classified clutter images) rates for each category.

Table 3.1: Number of training and test images used for the two-stage methods working on 10 categories

	Categories										
											Total
	1	2	3	4	5	6	7	8	9	10	Total
Number of training images											
Target	12	15	14	11	14	12	15	11	13	15	132
Clutter	12	15	14	11	14	12	15	11	13	15	132
Number of test images											
Target	140	338	304	213	321	142	358	275	194	342	2627
Clutter	1401	654	842	877	2924	1359	610	755	955	2969	13346

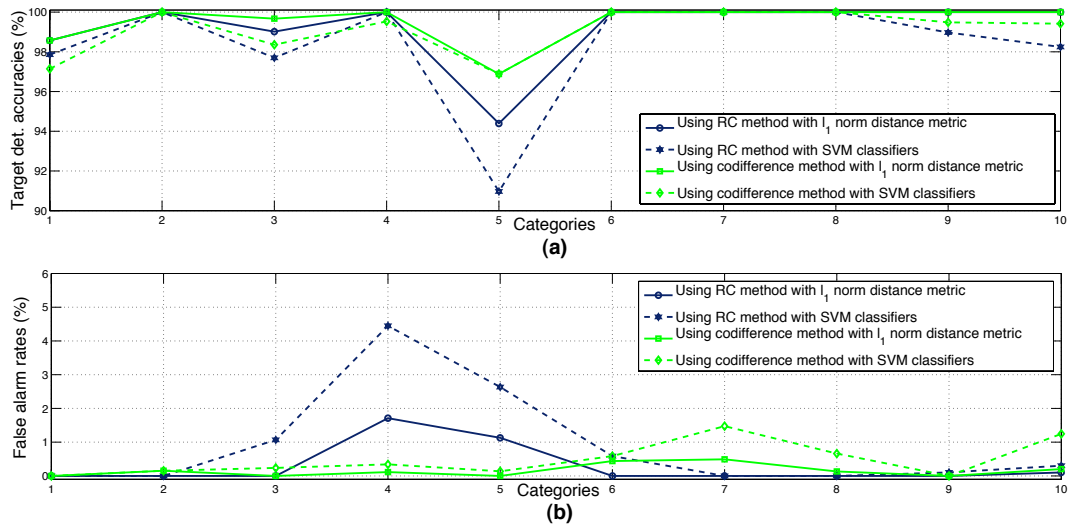





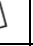




Figure 3.6: (a) Target detection accuracies (%) and (b) false alarm rates (%) obtained with the two-stage methods working on 10 categories

From Fig. 3.6 it is observed that when the images are distributed to 10 categories total target detection performances are degraded but they are still comparable to the results in Chapter 2. The general detection performance for target and clutter images rises when region codifference method is used instead of the RC method. Similarly, the decisions made with l_1 norm distance metric are better than the decision made using SVM classifiers.

The results in Fig. 3.6 also indicate that target detection accuracies are decreased and false alarm rates are increased for the decisions made in categories 5 and 10. To avoid this situation, categories 5 and 10 are simply eliminated. This leads the training images categorized in these categories to be distributed to the neighboring categories. It is assumed that the decision methods will produce better image classification performance if the training images in the neighboring categories are increased. Hence, by applying this procedure, the number of target and clutter training images in neighboring categories 4 and 9 are increased from 11 and 13 to 28 and 25, respectively as depicted in Table 3.2. The classification performances with 8 categories are given in Fig. 3.7.

Table 3.2: Number of training and test images used for the two-stage methods working on 8 categories

	Categories								Total
									
	1	2	3	4	6	7	8	9	
Number of training images									
Target	12	15	14	28	12	15	11	25	132
Clutter	12	15	14	28	12	15	11	25	132
Number of test images									
Target	140	338	305	541	142	358	276	527	2627
Clutter	1408	661	862	3750	1366	621	771	3907	13346

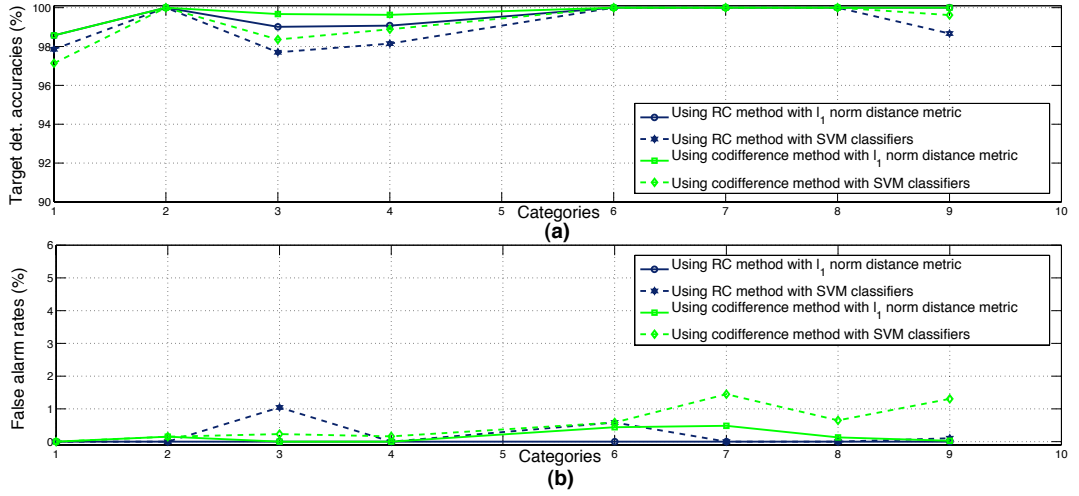





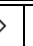
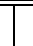


Figure 3.7: (a) Target detection accuracies (%) and (b) false alarm rates (%) obtained with the two-stage methods working on 8 categories

When the number of categories is reduced to 8, an improvement is achieved in target detection performance of the algorithm (see Fig. 3.7). The target detection accuracies are increased for all the two-stage methods. Besides, the total false alarm rates fall for most of the methods. Thus, 0% false alarm rate is achieved with l_1 norm distance comparisons on RC matrices. The rise in number of training images in categories 4 and 9 after eliminating the 5th and 10th category is the reason behind getting this better performance. Again, the results with region codifference method and l_1 norm distance metric are superior to the results obtained with RC method and SVM classifiers, respectively.

However, after examining Table 3.2 and Fig. 3.7, another step is still taken towards improving the performance of the algorithm by eliminating additionally the 1st category, as this category gives lower target detection rates than the other untouched categories, i.e. categories 2,3,6,7 and 8. The new simulation results on 7 categories are detailed in Fig. 3.8.

Table 3.3: Number of training and test images used for the two-stage methods working on 7 categories

	Categories							Total
								
	2	3	4	6	7	8	9	
Number of training images								
Target	25	14	28	14	15	11	25	132
Clutter	25	14	28	14	15	11	25	132
Number of test images								
Target	443	305	541	177	358	276	527	2627
Clutter	1358	880	3761	2028	630	775	3914	13346

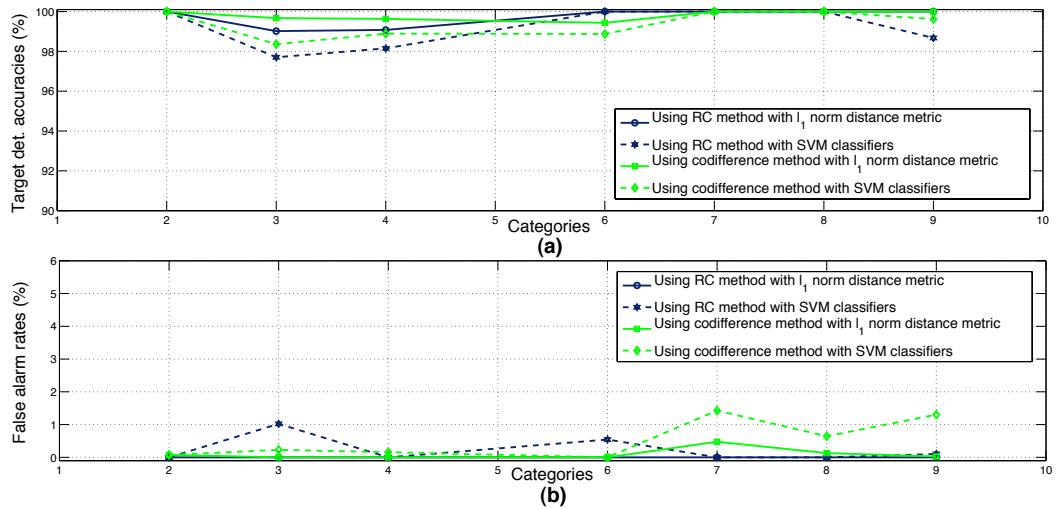




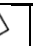



Figure 3.8: (a) Target detection accuracies (%) and (b) false alarm rates (%) obtained with the two-stage methods working on 7 categories

After eliminating the 1st category, the training images in this category are mostly moved to the 2nd category. The number of target and clutter training images in category 2 increased from 15 to 25, as in Table 3.3. Therefore, the target detection rates are increased in this category, eventually raising the total

detection accuracies. Furthermore, Fig. 3.8 suggests in general lower false alarm rates than the results obtained with 10 and 8 categories. If the categories are further restrained to 6 categories by eliminating the 6th category, the new target detection accuracies and false alarm rates will be as in Fig. 3.9.

Table 3.4: Number of training and test images used for the two-stage methods working on 6 categories

	Categories						
							
	2	3	4	7	8	9	Total
Number of training images							
Target	26	14	28	28	11	25	132
Clutter	26	14	28	28	11	25	132
Number of test images							
Target	477	305	541	501	276	527	2627
Clutter	2017	890	3770	1952	796	3921	13346

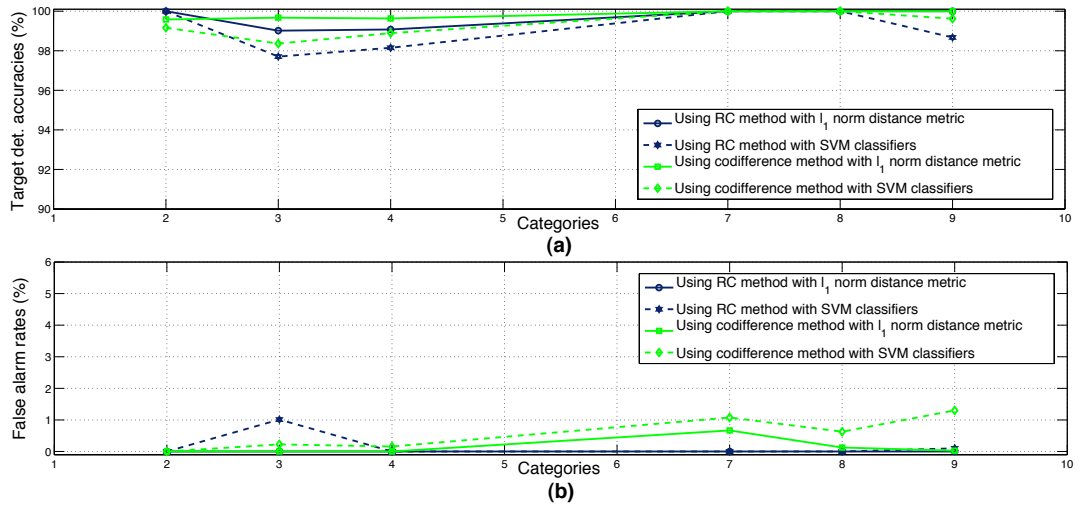







Figure 3.9: (a) Target detection accuracies (%) and (b) false alarm rates (%) obtained with the two-stage methods working on 6 categories

Unlike the results in Figures 3.7 and 3.8, the target detection results in Table 3.9 do not present an important performance improvement. As shown in Table 3.4, having still around 10 training images in some categories may be the reason behind these results.

To further improve the image classification performance, number of categories is restricted to 5 in the two-stage algorithm. In the new system, the number of training images in all categories is increased about twice of the number of training images provided in the simulation with original 10 categories in Table 3.1. Simulation results for this case are summarized in Fig. 3.10.

Table 3.5: Number of training and test images used for the two-stage methods working on 5 categories

	Categories					Total
						
	2	4	6	8	10	
Number of training images						
Target	31	30	20	27	24	132
Clutter	31	30	20	27	24	132
Number of test images						
Target	612	502	344	560	609	2627
Clutter	1765	2593	2383	1458	5147	13346

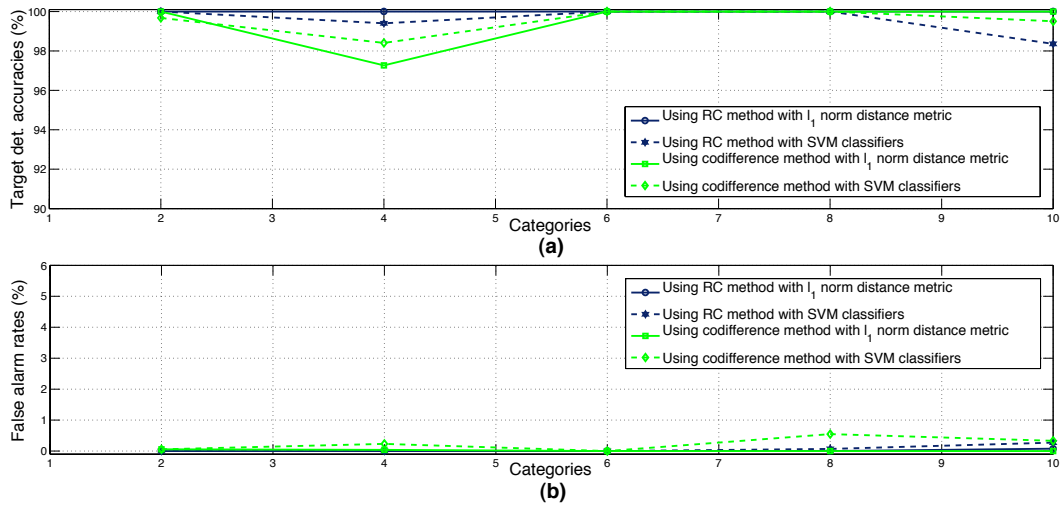










Figure 3.10: (a) Target detection accuracies (%) and (b) false alarm rates (%) obtained with the two-stage methods working on 5 categories

As noted in Table 3.5, the number of target and clutter images in each category is now at least 20. Thus this provides the first 100% detection rate with only 0.03% false alarm for the two-stage method using region covariance matrices with l_1 norm distance metric. The performance results with l_1 norm distance metric

and SVM classifiers got better compared to the previous cases with the increase in number of training images in the categories. However the rise in classification performance for the one-to-one matching methods using l_1 norms is larger than the methods using SVMs.

As the results until this point suggest, increasing the number of target and clutter training images by eliminating categories improved the target detection performance, especially for the RC and codifference methods working with the l_1 norm distance metric. Therefore the remaining three Tables 3.6, 3.7 and 3.8 and Figures 3.11, 3.12 and 3.13 present the SAR image classification results with 4, 3 and 2 categories respectively. The number of training images in the categories is increased gradually in these 3 simulations. It is observed that the total target detection accuracies and false alarm rates get better gradually with the increase in the number of training images in the categories. However, the classification performances are very close in Figures 3.12 and 3.13. The RC and codifference methods working with l_1 norm distance metric provide the highest detection and lowest false alarm rates. The performance of the RC method indicates that the classification gap is closed with the codifference method. For these 3 simulations using the two-stage algorithm, the results obtained with SVM classifiers are again worse than the results obtained using l_1 norm distance metric.

Table 3.6: Number of training and test images used for the two-stage methods working on 4 categories

	Categories									
					Total					Total
	2	4	7	9		2	4	7	9	
	Number of training images					Number of test images				
Target	32	36	32	32	132	646	677	648	656	2627
Clutter	32	36	32	32	132	2431	4246	2315	4354	13346

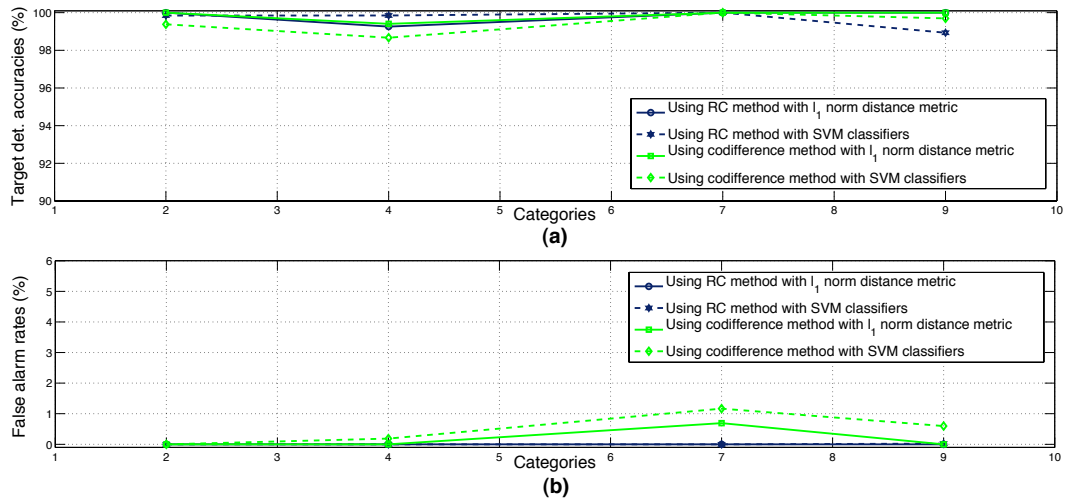








Figure 3.11: (a) Target detection accuracies (%) and (b) false alarm rates (%) obtained with the two-stage methods working on 4 categories

Table 3.7: Number of training and test images used for the two-stage methods working on 3 categories

	Categories							
				Total				Total
	3	6	9	Total	3	6	9	Total
	Number of training images				Number of test images			
Target	55	36	41	132	1066	604	957	2627
Clutter	55	36	41	132	3919	3259	6168	13346

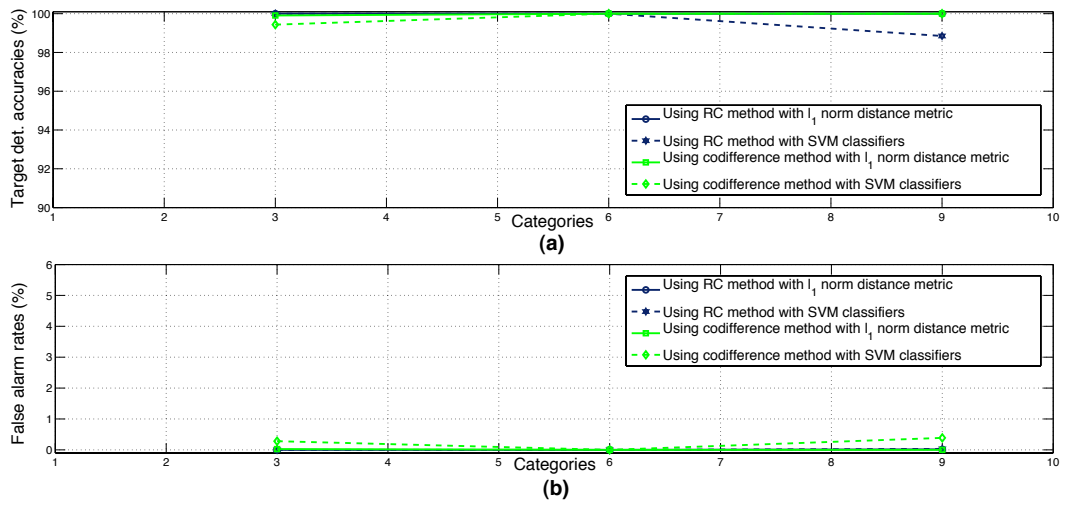


Figure 3.12: (a) Target detection accuracies (%) and (b) false alarm rates (%) obtained with the two-stage methods working on 3 categories

Table 3.8: Number of training and test images used for the two-stage methods working on 2 categories

	Categories					
	3	8	Total	3	8	Total
	Number of train. images			Number of test images		
Target	68	64	132	1331	1296	2627
Clutter	68	64	132	6682	6664	13346

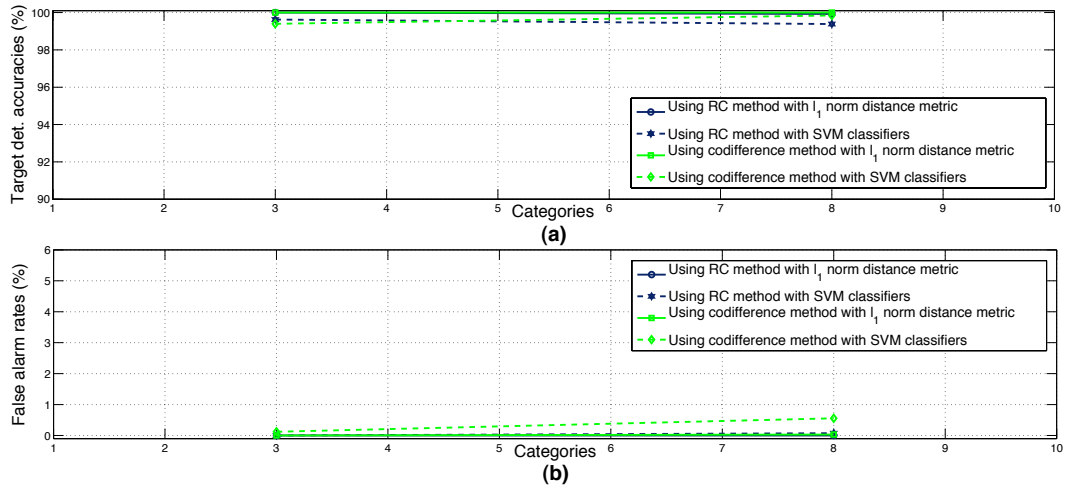


Figure 3.13: (a) Target detection accuracies (%) and (b) false alarm rates (%) obtained with the two-stage methods working on 2 categories

In Figures 3.14 and 3.15, the total target detection accuracies and false alarm rates are depicted respectively, for all variations of the categories. The results with only 1 category for training and test datasets, i.e. the results presented before in Tables 2.4 and 2.7 are also presented in the figures.

The results obtained using SVM and l_1 norm distance metric were close to each other in the old method in Chapter 2, especially when codifference method was used on the same 64-by-64 images as here. However, as it is seen from Fig. 3.14, the SVM classifiers miss more target images and mismatches more clutter images as the number of training images decreases with the increase in number of categories. The classification rates are much more accurate on the side of methods using l_1 norm distance metric. The plots for target detection accuracies also indicate that better target detection rates are achieved when region codifference methods are used instead of RC methods for almost all variations of the categories.

The RC method generally produces lower false alarm rates than the codifference method, as depicted in Fig. 3.15. However, in overall, the best detection

accuracies and the lowest false alarm rates that are highly comparable to the results in Chapter 2 are achieved using region codifference method with l_1 norm distance metric.

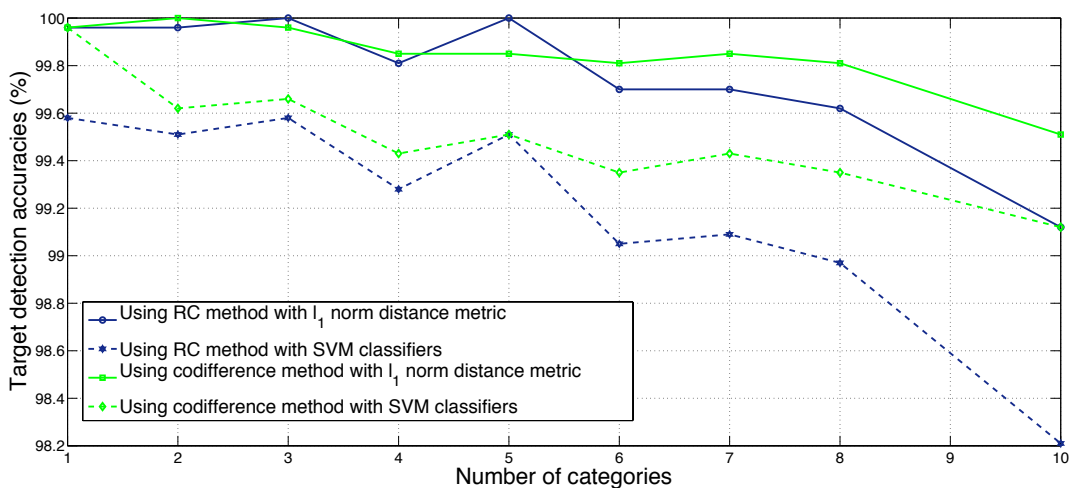


Figure 3.14: The total target detection accuracies (%) obtained with the two-stage RC and codifference methods using various decision techniques on different numbers of categories

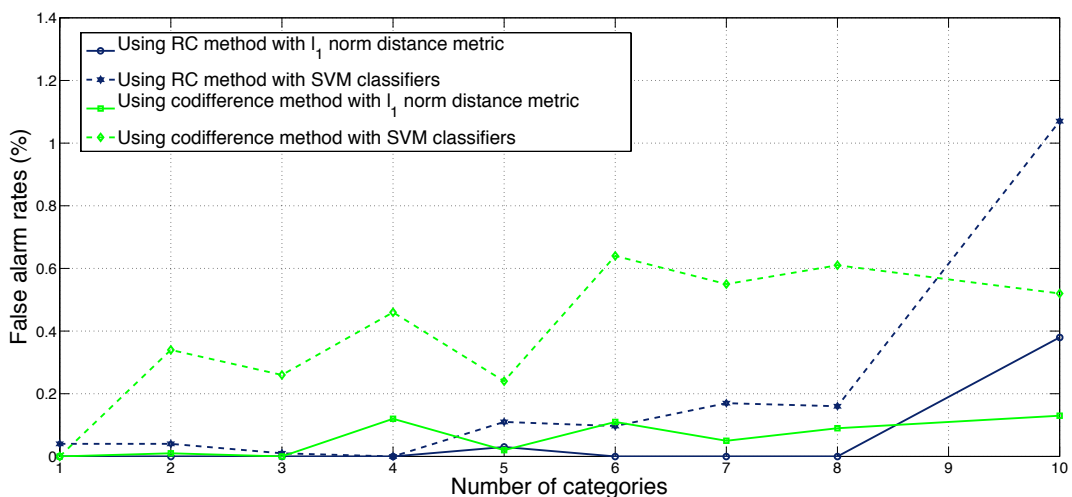


Figure 3.15: The total false alarm rates (%) obtained with the two-stage RC and codifference methods using various decision techniques on different numbers of categories

Further simulations are carried out with 10 categories by increasing or decreasing the number of target and clutter training images in each category. The results of these simulations are given in Table 3.9. The number of target and clutter training images used for these simulations change in between 5-10, 10-15, 15-20 and 20-25, respectively. The numbers of test images used are also given in the denominator part of the results. Increasing the number of training images increase the target detection accuracies generally, however it also leads to an increase in false alarm rates. This indicates that the target training images become dominant when the number of training images is increased for all target orientations.

Table 3.9: The total target detection accuracies and false alarm rates obtained with various numbers of training images on 10 categories

Number of training images in each category				
Target	5-10	10-15	15-20	20-25
Clutter	5-10	10-15	15-20	20-25
Simulation results				
Using RC method				
With l_1 norm distance metric				
Target det. accuracies	$\frac{2652}{2683}$ (98.84%)	$\frac{2604}{2627}$ (99.12%)	$\frac{2583}{2585}$ (99.92%)	$\frac{2532}{2539}$ (99.72%)
False alarm rates	$\frac{55}{13346}$ (0.41%)	$\frac{51}{13346}$ (0.38%)	$\frac{142}{13346}$ (1.06%)	$\frac{113}{13346}$ (0.85%)
With SVM classifiers				
Target det. accuracies	$\frac{2593}{2683}$ (96.65%)	$\frac{2580}{2627}$ (98.21%)	$\frac{2567}{2585}$ (99.30%)	$\frac{2525}{2539}$ (99.45%)
False alarm rates	$\frac{191}{13346}$ (1.43%)	$\frac{143}{13346}$ (1.07%)	$\frac{246}{13346}$ (1.84%)	$\frac{235}{13346}$ (1.76%)
Using reg. codifference method				
With l_1 norm distance metric				
Target det. accuracies	$\frac{2667}{2683}$ (99.40%)	$\frac{2614}{2627}$ (99.51%)	$\frac{2583}{2585}$ (99.92%)	$\frac{2536}{2539}$ (99.88%)
False alarm rates	$\frac{19}{13346}$ (0.14%)	$\frac{18}{13346}$ (0.13%)	$\frac{49}{13346}$ (0.37%)	$\frac{49}{13346}$ (0.37%)
With SVM classifiers				
Target det. accuracies	$\frac{2649}{2683}$ (98.73%)	$\frac{2604}{2627}$ (99.12%)	$\frac{2577}{2585}$ (99.69%)	$\frac{2531}{2539}$ (99.68%)
False alarm rates	$\frac{64}{13346}$ (0.48%)	$\frac{69}{13346}$ (0.52%)	$\frac{164}{13346}$ (1.23%)	$\frac{95}{13346}$ (0.71%)

3.4.1 Using k-Nearest Neighbor (k-NN) Algorithm

To increase the target detection performance of the two-stage system, the number of training images in each category is increased without eliminating any

categories. In this way, the number of target and clutter training images in 10 categories increased to a level between 20 and 25 images, as shown in Table 3.10.

Table 3.10: Number of training and test images used for the two-stage methods working on 10 categories of the new database

	Categories										
											Total
	1	2	3	4	5	6	7	8	9	10	Total
Number of training images											
Target	21	21	24	20	23	21	24	22	20	24	220
Clutter	21	21	24	20	23	21	24	22	20	24	220
Number of test images											
Target	131	332	294	204	312	133	349	264	187	333	220
Clutter	1429	667	852	877	2868	1374	618	758	956	2947	13346

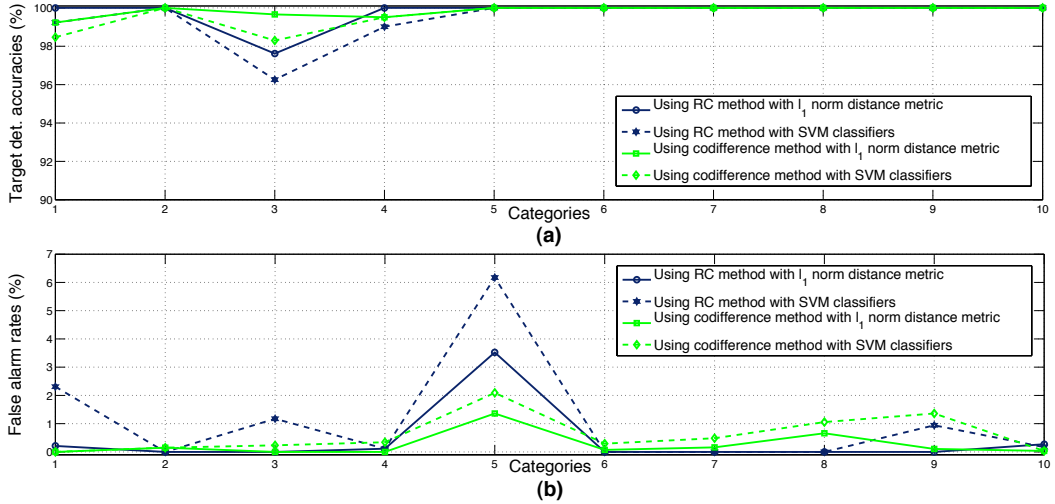


Figure 3.16: (a) Target detection accuracies (%) and (b) false alarm rates (%) obtained with the two-stage methods working on 10 categories of the new database

According to the results in Figures 3.16 and 3.6, as in Table 3.9, it is again possible to observe that increasing the number of target and clutter training images without reducing the number of categories produces higher target detection accuracies but this also leads to higher false alarm rates.

The $K - NN$ algorithm is also applied on the two-stage system similar to the previous chapter. Decisions are reached again from the first k RC or codifference matrices that produce the smallest l_1 norm distance with the 64-by-64 images.

As noted in Table 3.10, the minimum number of training images is 20 with the new database. Therefore, the target detection results are collected with a range of values as $k = \{1, 5, 10, 15, 20\}$ for all 10 available categories. The following Figures 3.17 and 3.18 respectively show the total target detection accuracies and false alarm rates in percentages achieved with these k values.

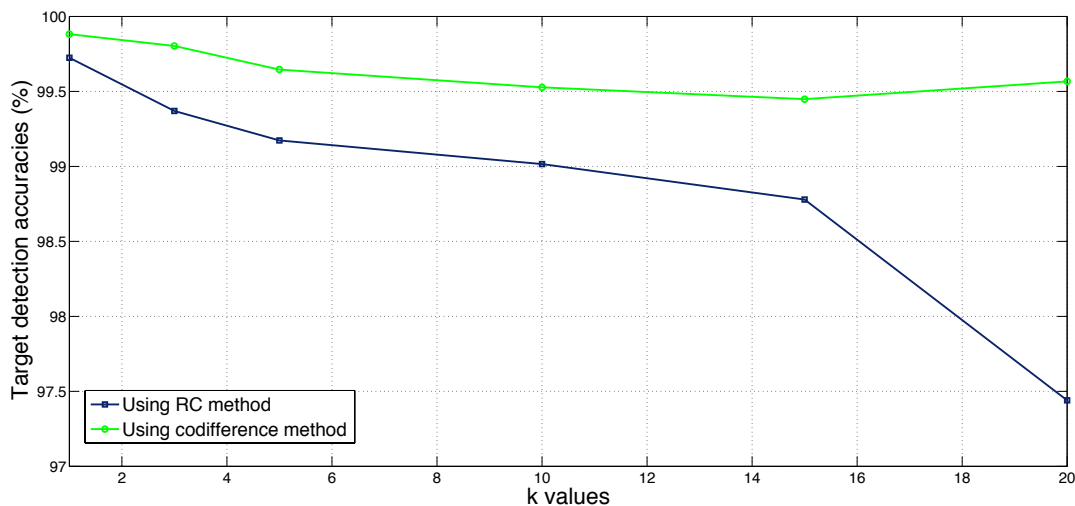


Figure 3.17: The total target detection accuracies (%) obtained for increasing k values on 10 categories for the two-stage system using l_1 norm distance metric.

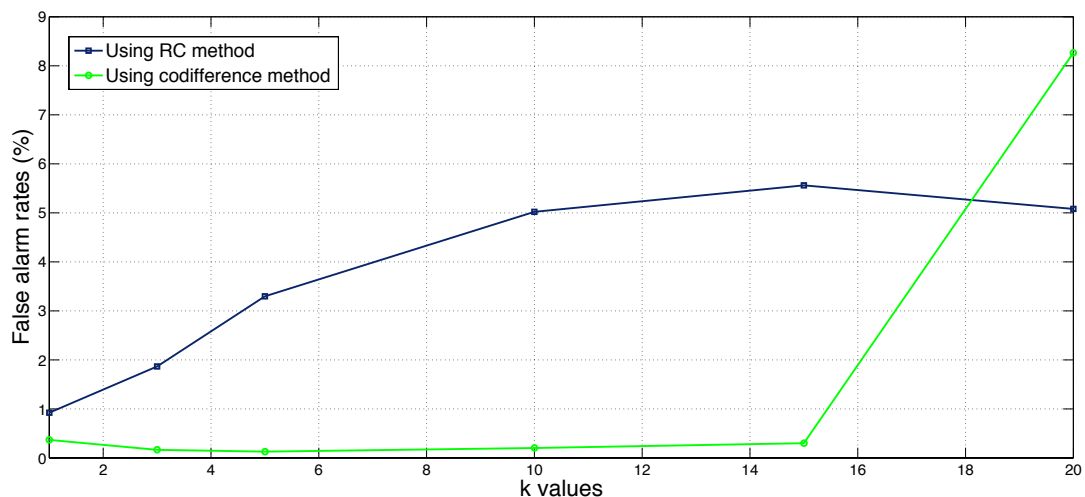


Figure 3.18: The total false alarm rates (%) obtained for increasing k values on 10 categories for the two-stage system using l_1 norm distance metric.

As shown in Fig. 3.17, when k values are increased, the target detection accuracies of the RC and codifference methods decrease gradually, however the degradation is more severe in the RC method.

False alarm rates also increase when using the RC method with increase in k values, as illustrated in Fig. 3.18. These rates stay stable for $k = \{1, 5, 10, 15\}$ when codifference features are used, however they do a peak when $k = 20$.

As a result, using $k - NN$ algorithm on the two-stage system is inaccurate both from the computational cost and detection performance points of view, similar to the method described in Section 2.6.1.

3.5 Summary

The use of directional filters with the region covariance (RC) and codifference method to detect targets in SAR images is described in this chapter. Directional filtering makes it possible to classify target and clutters into different subcategories according to their geometrical orientations. As the target detection results presented in this chapter shows, computational cost of the earlier algorithm in Chapter 2 is significantly reduced without losing much from the classification performance of the system when l_1 norm distance metric is used either with the RC or codifference method. Decisions on target and clutter images using SVM classifiers in the two-stage system produce worse SAR image classification results than decisions made using l_1 norm distance metric. In addition, the two-stage algorithm with SVM classifiers has the same computational cost with the single-stage method described in the previous chapter.

Chapter 4

Conclusions

In this thesis, a descriptive feature parameter extraction technique from SAR images is proposed. This approach is based on region covariance (RC) method which involves computation of a covariance matrix whose entries can be used in target detection and discrimination stages of a typical ATR system. In addition, the region codifference matrix is also introduced for SAR image classification. Computation of the codifference matrix is more efficient than the RC matrix.

Porikli et. al. used generalized eigenvalue based distance measure to compare two covariance matrices in [12]. Difference of distinct eigenvalues is also used as a distance metric instead of this measure. However, extracting eigenvalues is computationally costly. Therefore, distance between two covariance or codifference feature vectors of the training and test images are computed using various distance metrics and SVM classifiers.

To decrease the computational complexity further, directional filters (DFs) are used as a pre-processing stage which divide the training and test images into categories. These categories restrict the search spaces for tested images. The number of distance comparisons between RC and codifference features is reduced with the introduced pre-processing method. That is how the cost of the

detection algorithm is decreased. Simulation results for the proposed algorithms are tested with the only publicly available SAR database, MSTAR SAR database.

RC and codifference algorithms are applied to 128-by-128 and 64-by-64 pixel sized target and clutter SAR images. The proposed RC and codifference algorithms are shown to deliver high detection accuracies and low false alarm rates, although the codifference matrix based methods often provide better detection performance than the RC matrix based methods. In general, the detection results presented in Chapter 2 are close to each other for both 128-by-128 and 64-by-64 images. For 64-by-64 images, better detection performances are achieved by these methods than the commonly used PCA method.

The distance metrics involving l_1 norms with and without normalizations produce best detection results. However, Porikli's distance metric also provided close classification performance to these distance measures. Simulations indicate that a measure based on logarithmic differences between the eigenvalues of the RC and codifference matrices leads to the worst detection results. The $k - NN$ algorithm is used also with the l_1 norm distance metric. However, in most cases, classification performances are degraded with growing k values.

Training and testing the covariance and codifference features using SVMs, which rely on the use of Euclidean distance, also provide close detection rates to the results achieved using distance measures based on l_1 norms.

In order to reduce the number of comparisons, the methods proposed in the first part of the thesis are applied on the categories of images produced by the pre-processing stage consisting of directional filters. This time the computationally efficient l_1 norm distance metric and the SVM classifiers are used in order to discriminate between target and clutter images within the categories, which have much lower number of training images than the previous case. Hence, the number of calculated distances using l_1 norm is decreased drastically leading to

less computational cost for the overall SAR classification system. It is again observed that the region codifference features work better than RC features in describing ROIs. Similarly, the l_1 norm distance metric works better than the SVM classifiers. Therefore, the codifference method with l_1 norm produces the highest target detection accuracy with lowest false alarm rates and low computational cost, as in the single-stage system. The $k - NN$ algorithm is also tried on the two-stage system but it produced unsatisfactory detection results.

For real-time applications, the SAR image classification method based on SVM using codifference features has the lowest computational complexity. Its image classification accuracy is close to the l_1 norm distance based classification.

Bibliography

- [1] J. C. Curlander and R. N. McDonough, *Synthetic Aperture Radar - Systems and Signal Processing*. John Wiley & Sons, Inc., New York, 1991.
- [2] C. Oliver and S. Quegan, *Understanding Synthetic Aperture Radar Images*. Scitech Publishing, Inc., Raleigh, NC, 2004.
- [3] “Sandia National Laboratories.” <http://www.sandia.gov/>.
- [4] L. M. Novak, G. J. Owirka, and C. M. Netishen, “Performance of a high-resolution polarimetric SAR automatic target recognition system,” *The Lincoln Laboratory Journal*, vol. 6, no. 1, pp. 11–24, 1993.
- [5] L. M. Novak, G. J. Owirka, W. S. Brower, and A. L. Weaver, “The automatic target-recognition system in SAIP,” *The Lincoln Laboratory Journal*, vol. 10, no. 2, pp. 187–202, 1997.
- [6] H.-C. Chiang, R. L. Moses, and L. C. Potter, “Model-based classification of radar images,” *IEEE Transactions on Information Theory*, vol. 46, pp. 1842–1854, Aug. 2000.
- [7] L. M. Novak, G. J. Owirka, and A. L. Weaver, “Automatic target recognition using enhanced resolution SAR data,” *IEEE Transactions on Aerospace and Electronic Systems*, vol. 35, pp. 157–175, Jan. 1999.
- [8] L. M. Novak, “State-of-the-art of SAR automatic target recognition,” in *Proc. of the IEEE International Radar Conference*, pp. 836–843, May 2000.

- [9] Q. Zhao and J. C. Principe, “Support vector machines for SAR automatic target recognition,” *IEEE Transactions on Aerospace and Electronic Systems*, vol. 37, pp. 643–654, April 2001.
- [10] C. Nilubol, Q. H. Pham, R. M. Mersereau, M. J. T. Smith, and M. A. Clements, “Hidden markov modelling for SAR automatic target recognition,” in *Proc. of the IEEE International Conference on Acoustics, Speech and Signal Processing (ICASSP '98)*, vol. 2, pp. 1061–1064, May 1998.
- [11] S. A. Stanhope and J. M. Daida, “Genetic programming for automatic target classification and recognition in synthetic aperture radar imagery,” *Evolutionary Programming VII*, pp. 735–744, 1998.
- [12] O. Tuzel, F. Porikli, and P. Meer, “Region covariance: A fast descriptor for detection and classification,” in *Proc. of the European Conference on Computer Vision (ECCV '06)*, pp. 367–379, May 2006.
- [13] O. Tuzel, F. Porikli, and P. Meer, “Human detection via classification on riemannian manifolds,” in *Proc. of the IEEE Conference on Computer Vision and Pattern Recognition (CVPR '07)*, pp. 1–8, June 2007.
- [14] F. Porikli and T. Kocak, “Robust license plate detection using covariance descriptor in a neural network framework,” in *Proc. of the IEEE International Conference on Video and Signal Based Surveillance (AVSS '06)*, Nov. 2006.
- [15] F. Porikli, O. Tuzel, and P. Meer, “Covariance tracking using model update based means on riemannian manifolds,” in *Proc. of the Computer Vision and Pattern Recognition Conference (CVPR '06)*, vol. 1, pp. 728–735, June 2006.
- [16] Center for Imaging Science (CIS), “MSTAR (Moving and Stationary Target Recognition) SAR database.” <http://cis.jhu.edu/data.sets/MSTAR/>.

- [17] C. Wang and X. Zhong, “Analysis of man-made target detection in SAR imagery,” in *Envisat Symposium*, April 2007.
- [18] F. Porikli and O. Tuzel, “Fast construction of covariance matrices for arbitrary size image windows,” in *Proc. of the IEEE International Conference on Image Processing (ICIP '06)*, pp. 1581–1584, Oct. 2006.
- [19] T. Akgul, M. Sun, R. J. Scilahassi, and A. E. Cetin, “Characterization of sleep spindles using higher order statistics and spectra,” *IEEE Transactions on Biomedical Engineering*, vol. 47, pp. 997–1009, Aug. 2000.
- [20] I. T. Jolliffe, *Principal Component Analysis*. Springer, Second Ed., Oct. 2002.
- [21] C.-C. Chang and C.-J. Lin, “LIBSVM: a library for support vector machines.” <http://www.csie.ntu.edu.tw/~cjlin/libsvm/>, 2001.
- [22] K. Duman, A. Eryildirim, and A. E. Cetin, “Target detection and classification in SAR images using region covariance and co-difference,” in *Proc. of the Society of Photo-Optical Instrumentation Engineers (SPIE) Conference*, vol. 7337, May 2009.
- [23] B. Ramamurthi and A. Gersho, “Classified vector quantization of images,” *IEEE Transactions on Communications*, vol. 34, pp. 1105–1115, Nov. 1986.
- [24] O. N. Gerek and A. E. Cetin, “A 2-D orientation-adaptive prediction filter in lifting structures for image coding,” *IEEE Transactions on Image Processing*, vol. 15, pp. 106–111, Jan. 2006.
- [25] M. N. Do and M. Vetterli, “The contourlet transform: an efficient directional multiresolution image representation,” *IEEE Transactions on Image Processing*, vol. 14, no. 12, pp. 2091–2106, 2005.

- [26] G. Peyre and S. Mallat, “Discrete bandelets with geometric orthogonal filters,” in *Proc. of the IEEE International Conference on Image Processing (ICIP '05)*, vol. 1, pp. I-65-8, Sept. 2005.
- [27] P. Viola and M. Jones, “Robust real-time face detection,” *International Journal of Computer Vision*, vol. 57, pp. 137-154, 2004.